

Revitalizing Black-Box Interpretability: Actionable Interpretability for LLMs via Proxy Models

Junhao Liu, Haonan Yu, Zhenyu Yan, Xin Zhang*

Key Lab of High Confidence Software Technologies (Peking University), Ministry of Education
School of Computer Science, Peking University, Beijing, China
{liujunhao, xin}@pku.edu.cn, {haonanyu, zhenyuyan}@stu.pku.edu.cn

Abstract

Post-hoc explanations provide transparency and are essential for guiding model optimization, such as prompt engineering and data sanitation. However, applying model-agnostic techniques to Large Language Models (LLMs) is hindered by prohibitive computational costs, rendering these tools dormant for real-world applications. To revitalize model-agnostic interpretability, we propose a budget-friendly proxy framework that leverages efficient models to approximate the decision boundaries of expensive LLMs. We introduce a screen-and-apply mechanism to statistically verify local alignment before deployment. Our empirical evaluation confirms that proxy explanations achieve over 90% fidelity with only 9.5% of the oracle’s cost. Building on this foundation, we demonstrate the actionable utility of our framework in prompt compression and poisoned example removal. Results show that reliable proxy explanations effectively guide optimization, transforming interpretability from a passive observation tool into a scalable primitive for LLM development. Additionally, we open-source code and datasets to facilitate future research¹.

1 Introduction

Post-hoc explanations are not only passive transparency tools, they are also drivers for active model optimization (Shin et al., 2020; Tenney et al., 2024). However, the ubiquity of closed-source models like GPT-4o (OpenAI et al., 2024) and Google Gemini (Google et al., 2025) blocks access to internal representations. This renders model-agnostic methods the only viable option, but their reliance on massive sampling renders them economically impractical for real-world deployment. In this work, we propose a budget-friendly proxy framework to revitalize model-agnostic interpretability for LLM.

*Corresponding author.

¹The code and datasets are available at <https://github.com/outerform/XLLM-Bench>

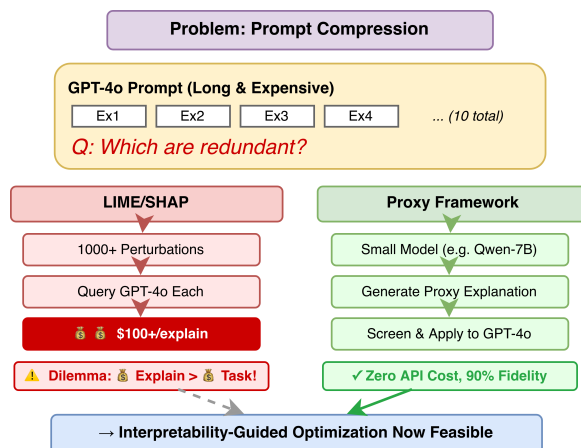


Figure 1: The dilemma of using model-agnostic explanation methods to optimize expensive LLMs.

Let us consider an example of interpretability-guided prompt compression as shown in Figure 1. An LLM user aims to reduce the inference cost by removing redundant few-shot examples from a lengthy prompt template. Ideally, feature attribution methods like LIME (Ribeiro et al., 2016) could identify which examples contribute least to the model’s predictions. Specifically, generating a single LIME explanation typically requires querying the target model with thousands of perturbed samples (e.g., 1,000). Consequently, to evaluate the effectiveness of each prompt compression strategy, the user would need to generate explanations on a validation set of multiple examples (e.g., 50), leading to an exorbitant number of model invocations. As detailed in Table 1, querying GPT-4o for explanations on a small validation set of 50 examples would require 50,000 queries costing upwards of \$100. Besides the high cost itself, this also creates a fundamental utility dilemma: the upfront cost of generating explanations dwarfs the potential savings from the optimization task itself, effectively keeping these powerful tools dormant.

To address this limitation, we propose a budget-

friendly proxy explanation framework to generate model-agnostic explanations for expensive LLMs.

Our approach is motivated by the homogeneity among LLMs (Jiang et al., 2025; Lee et al., 2025). This indicates that smaller, cost-efficient models can also potentially have similar local decision boundaries as their larger counterparts, allowing us to *see the big in the small*. Specifically, instead of querying the expensive oracle, we generate perturbation-based explanations using local, efficient models (e.g., open-source Qwen (Yang et al., 2025) or LLaMA (Grattafiori et al., 2024) models) as budget-friendly proxies. Crucially, strictly relying on small models introduces risks of misalignment. To ensure reliability, we introduce a **screen-and-apply** framework: before applying a proxy explanation, a statistical screening step verifies whether the proxy model’s local decision boundary aligns with the target model. This acts as a safety valve, ensuring we only deploy budget-friendly explanations when they are faithful to the expensive model’s behavior.

We validate our framework through a comprehensive empirical study spanning 12 state-of-the-art LLMs—ranging from open-source models like LLaMA 3.1 (Grattafiori et al., 2024) and DeepSeek V3 (DeepSeek-AI et al., 2025) to proprietary giants like GPT-4o—across seven diverse tasks including the MMLU benchmark (Hendrycks et al., 2020). The results confirm that budget-friendly proxies can serve as faithful surrogates, achieving over 90% fidelity to oracle explanations while reducing economic costs by 90.5%. Building on this foundation, we further demonstrate the actionable utility of our framework on downstream optimization tasks: proxy-guided pruning effectively compresses prompts for GPT-4o without performance loss, and proxy explanations accurately identify poisoned examples without accessing the target model.

Contributions. The main contributions of this work are summarized as follows:

- We propose a novel proxy-based framework to **revitalize** model-agnostic interpretability for LLMs. By introducing a statistical **screen-and-apply** mechanism, we enable the reliable use of budget-friendly models to approximate the local decision boundaries of expensive, closed-source LLMs.
- We conduct an extensive two-stage evaluation across 12 state-of-the-art LLMs. Our results

demonstrate that proxy explanations achieve over 90% fidelity with a 90.5% cost reduction, and also show their actionable utility in downstream applications. We show that proxy explanations effectively guide prompt compression and poisoned example removal.

- We release **XLLM-Bench**, a comprehensive dataset containing perturbation samples and model outputs collected from our study, serving as a foundation for future research on efficient LLM interpretability.

2 Background and Related Work

In this section, we review the background of model-agnostic interpretability and discuss existing limitations that hinder its application for LLM optimization.

2.1 Large Language Models and Their Homogeneity

We consider a large language model (LLM) as a probabilistic function f that maps an input sequence of tokens $\mathbf{x} = [x_1, x_2, \dots, x_n]$ to a probability distribution over the vocabulary \mathcal{V} , denoted as $f(\mathbf{x}) \in \mathbb{R}^{|\mathcal{V}|}$. While LLM architectures vary, recent research reveals the homogeneity among state-of-the-art LLMs (Jiang et al., 2025; Lee et al., 2025; Zhou et al., 2024; Wright et al., 2025), i.e., different LLMs tend to behave similarly on similar inputs in many scenarios. This observation motivated our methodology.

2.2 Model-Agnostic Explanations

A local model-agnostic explanation technique t takes a predictive model f and an instance \mathbf{x} as input, returning an attribution vector $\mathbf{a} \in \mathbb{R}^n$ that quantifies the contribution of each input token to the prediction $f(\mathbf{x})$. Representative methods like LIME (Ribeiro et al., 2016), SHAP (Lundberg and Lee, 2017), and their variants (Paes et al., 2024; Enouen et al., 2024; Luss et al., 2024; Hackmann et al., 2024; Liu and Zhang, 2025; Liu et al., 2026b,a; Yu et al., 2026) estimate these attributions by querying f with a large set of perturbed samples $\mathcal{Z} = \{z_1, \dots, z_k\}$ sampled from the local neighborhood of \mathbf{x} .

While effective, generating a single reliable explanation typically requires thousands of queries. For API-based models like GPT-4o, the accumulated cost of these queries renders standard applications economically prohibitive.

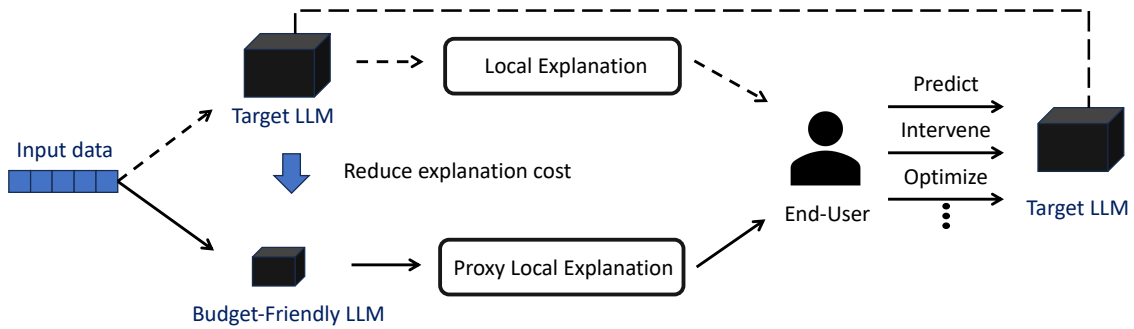


Figure 2: The workflow for leveraging proxy explanations from budget-friendly models to reduce the cost of explaining expensive LLMs.

Several studies have also focused on reducing the cost of generating post-hoc model-agnostic explanations. As surveyed by [Chuang et al. \(2023a\)](#), some methods amortize explanation generation across inputs by training a unified explainer to approximate the distribution of model explanations ([Covert et al., 2024](#); [Jethani et al., 2022](#); [Chuang et al., 2023b](#); [Chen et al., 2018](#)). Other approaches remain non-amortized and generate explanations on a per-instance basis, but aim to improve efficiency through various strategies. These include reducing the number of features in the explanation ([Chen et al., 2018](#); [Yoon et al., 2019](#); [Wang et al., 2022](#); [Jullum et al., 2021](#)), optimizing the perturbation process ([Mitchell et al., 2022](#); [Dandolo et al., 2023](#)), or leveraging global dataset-level information ([Yu et al., 2026](#)). These methods are orthogonal to our approach and can be integrated with it to further reduce the cost of explanation generation.

Desiderata of Explanations **Fidelity** and **understandability** are two key desiderata for local explanations aimed at end-users ([Dwivedi et al., 2023](#); [Zhang et al., 2021](#); [Rojat et al., 2021](#); [Mahto, 2024](#)).

On one hand, explanations should faithfully reflect the model’s decision-making process. High fidelity indicates that the explanation accurately captures how the model arrives at its predictions. On the other hand, explanations should be understandable—that is, they should be presented in a form that humans can easily interpret.

In this paper, we conduct our empirical studies using attribution-based techniques, which produce simple and understandable forms of explanation. Therefore, we focus our evaluation on the **fidelity** of proxy explanations generated by budget-friendly models.

2.3 Explanations for Prompt Optimization

Beyond transparency, post-hoc explanations are increasingly recognized as powerful drivers for active model optimization, such as prompt debugging or compression.

Some works have explored how explanations can help optimize LLMs. However, existing works either use white-box explanations that require access to model internal representations ([Tenney et al., 2024](#); [Shin et al., 2020](#)), or only focus on specific tasks or model settings ([Zhao et al., 2025](#); [Jiang et al., 2023](#)). This limits their applicability in real-world scenarios.

In contrast, our method uses proxy model-agnostic explanations as a general and scalable tool to optimize LLMs in a budget-friendly manner.

3 Proxy Explanation Framework

In this section, we introduce the proxy explanation framework. Our approach is motivated by the homogeneity among LLMs as discussed in Section 2.1. While homogeneity holds generally, it is not guaranteed for every instance. Blindly applying proxy explanations introduces risks of misalignment. Thus, we propose a **screen-and-apply** framework consisting of two key steps: (1) a screening step to determine if proxy explanations can be reliably used for current tasks or instances, and (2) applying the proxy explanations to generate faithful explanations for the target expensive LLMs.

3.1 Screening Step

We use a two-stage screening to ensure proxy explanations from a budget-friendly model f' are reliable for an expensive LLM f on a task or dataset with input set \mathbb{D} using a local technique t . For simplicity, we treat both models as deterministic functions mapping an input x to a prediction $f(x)$

or $f'(\mathbf{x})$. Specifically, the screening procedure includes: an offline task-level screening and an online instance-level screening. 1) The task-level screening is performed once per task. It assesses whether f' can provide sufficiently faithful proxy explanations for f over the entire input set \mathbb{D} , offering a task-level fidelity assessment. 2) The instance-level screening is a lightweight runtime check applied to each input \mathbf{x} . It verifies whether f' and f agree on the prediction for \mathbf{x} .

Task-Level Screening (Offline) Given a target LLM f , a dataset or task with input set \mathbb{D} , and an explanation technique t , we run task-level screening once to ensure that proxy explanations from a budget-friendly model f' are on average sufficiently faithful. Specifically, we perform statistical hypothesis testing to check whether the proxy explanations from f' achieve at least a fraction τ of the fidelity of oracle explanations from f , with confidence level $1 - \delta$. Formally, we define the task-level screening decision as a binary function: $s_{\text{task}}^{\tau, \delta}(\mathbb{D}; f, f') \in \{0, 1\}$. To keep consistent with the instance-level screening, we only consider inputs on which f and f' agree: $\mathbb{D}' = \{\mathbf{x} \in \mathbb{D} : f(\mathbf{x}) = f'(\mathbf{x})\}$, from which we draw samples via rejection sampling. Let $q_{\text{proxy}}(\mathbf{x})$ and $q_{\text{oracle}}(\mathbf{x})$ denote the (per-instance) fidelities on \mathbb{D}' of proxy and oracle explanations, respectively (as defined in Section 4.2). We conduct a *sequential one-sided paired t-test* on the paired differences

$$d_i = q_{\text{proxy}}(\mathbf{x}_i) - \tau q_{\text{oracle}}(\mathbf{x}_i), \quad i = 1, \dots, n,$$

and test

$$H_0 : \mu_d < 0 \quad \text{vs.} \quad H_1 : \mu_d \geq 0,$$

where $\mu_d = \mathbb{E}[d_i]$ is the population mean difference on \mathbb{D}' . At step n we update the sample mean and variance of the paired differences,

$$\bar{d} = \frac{1}{n} \sum_{i=1}^n d_i, \quad s_d^2 = \frac{1}{n-1} \sum_{i=1}^n (d_i - \bar{d})^2.$$

After each new paired sample, we compute a $(1 - \delta)$ confidence interval for $\mu_d = \bar{q}_{\text{proxy}} - \tau \bar{q}_{\text{oracle}}$ as

$$\left(\bar{d} - t_{\nu, 1-\delta/2} \frac{s_d}{\sqrt{n}}, \quad \bar{d} + t_{\nu, 1-\delta/2} \frac{s_d}{\sqrt{n}} \right),$$

where $t_{\nu, 1-\delta/2}$ is the $1 - \delta/2$ quantile of the t -distribution with $\nu = n - 1$ degrees of freedom.

If the entire interval lies above zero, we accept H_1 ; if it lies entirely below zero, we accept H_0 . Otherwise, we continue sampling until a confident decision is reached or a maximum sample size N is exhausted. Finally, if H_1 is accepted, we set $s_{\text{task}}^{\tau, \delta}(f'; f, \mathbb{D}) = 1$, indicating that proxy explanations from f' are sufficiently faithful on average for \mathbb{D} ; otherwise, we set $s_{\text{task}}^{\tau, \delta}(f'; f, \mathbb{D}) = 0$.

Instance-Level Screening (Online) If f' passes the task-level screening, we apply an instance-level check for each input \mathbf{x} to filter out cases where the two models disagree. For a given \mathbf{x} , the instance-level screening function is

$$s_{\text{inst}}(\mathbf{x}; f, f') = \mathbf{1}[f(\mathbf{x}) = f'(\mathbf{x})].$$

The rationale is twofold: (1) local explanations are designed for the model’s current prediction, so proxy explanations are appropriate only when the two models agree; and (2) disagreement suggests different local decision behavior around \mathbf{x} , making proxy explanations more likely to be unfaithful.

3.2 Applying Proxy Explanations

If the budget-friendly model f' passes the task-level screening, and the input instance \mathbf{x} passes the instance-level screening, our framework will apply the proxy explanations from f' , i.e., $t(f', \mathbf{x})$, to explain the behavior of the expensive LLM f around \mathbf{x} .

For more details, please refer to Appendix C.

4 Fidelity Evaluation

In this section, we first introduce the experimental setup used in our empirical studies, and then present and analyze results to answer the following research questions:

1. **Cost Reduction:** To what extent can the proposed proxy explanation framework reduce the cost of generating explanations for expensive LLMs? This is the primary focus of our study.
2. **Screening Reliability:** How reliable is the screening step in our framework? This checks if the screening step is necessary and sufficient to ensure the fidelity of proxy explanations.
3. **Proxy Explanation Generalizability:** Does the transferability of explanations across models hold consistently across different tasks and datasets? This aspect is crucial for demonstrating the generalizability and applicability of our method.

Table 1: Common LLM Official API pricing (USD per million tokens). Specifically, Qwen 2.5 models with 0.5B and 1.5B parameters can be accessed from Alibaba (https://www.aliyun.com/) for **free**, and all open-source models with 8B or fewer parameters can be run locally on a single consumer-grade GPU.

Model	Provider	Input	Output	Open-source
GPT-4o	OpenAI	\$2.50	\$10.00	No
GPT-4o Mini	OpenAI	\$0.15	\$0.60	No
DeepSeek V3	DeepSeek	\$0.27	\$1.10	Yes
Qwen 2.5 0.5B	Alibaba	–	–	Yes
Qwen 2.5 1.5B	Alibaba	–	–	Yes
Qwen 2.5 3B	Alibaba	\$0.04	\$0.12	Yes
Qwen 2.5 7B	Alibaba	\$0.07	\$0.14	Yes
Qwen 2.5 14B	Alibaba	\$0.14	\$0.41	Yes
Qwen 2.5 32B	Alibaba	\$0.28	\$0.83	Yes
Qwen 2.5 72B	Alibaba	\$0.56	\$1.67	Yes
LLaMA 3.1 8B	Meta	\$0.18	\$0.18	Yes
LLaMA 3.1 70B	Meta	\$0.88	\$0.88	Yes

4.1 Experimental Setup

4.1.1 Target Models and Explanation Techniques

We conducted our experiments on 12 popular generative language models, including two from the GPT-4o series, DeepSeek V3, seven Qwen 2.5 models, and two Llama 3.1 models, as listed in Table 1. We accessed GPT-4o series and DeepSeek V3 via their official APIs, while running the other models locally.

The models were selected based on their popularity, as well as diversity in architecture, size, and pricing. They cover both dense and Mixture-of-Experts (MoE) architectures, parameter counts ranging from 0.5 billion (Qwen2.5-0.5B) to 685 billion (DeepSeek V3). Their associated costs vary significantly: GPT-4o is the most expensive at \$2.50 per million input tokens and \$10.00 per million output tokens, while Qwen2.5-0.5B is the most affordable, whose official APIs are currently free and can also be deployed locally on a single consumer-grade GPU with minimal computational costs.

We use two representative attribution-based explanation techniques: LIME (Ribeiro et al., 2016) and Kernel SHAP (Lundberg and Lee, 2017), to generate local explanations. For both methods, we set the number of perturbation samples to 1,000 and use default values for all other hyperparameters. When applying our proxy explanation framework, we set the dataset-level screening threshold $\tau = 0.9$ and confidence level $1 - \delta = 0.95$, and a maximum sample size $N = 50$. We provide a sen-

sitivity analysis on hyperparameters in Section 4.3.

4.1.2 Tasks and Datasets

We evaluate our approach on three representative tasks: sentiment analysis, multiple-choice question answering, and text generation, where sentiment analysis is a classic task in studying model explanations, multiple-choice question answering is a common benchmark for evaluating the performance of LLMs, and text generation is a widely used task of LLMs beyond classification. Considering the budget limitation, we select one dataset from each task to analyze the effectiveness of using proxy explanations. Besides, we conduct our experiments on another three datasets to further validate whether the cross-model explanation transferability holds across different datasets.

Sentiment Analysis We use the Stanford Sentiment Treebank (SST) dataset (Socher et al., 2013) for classification. Following the standard train/validation/test split, we generate explanations for all 2,210 sentences in the test set. The target model is prompted in a zero-shot setting to predict whether the sentiment of a given sentence is positive or negative.

Multiple-Choice Question Answering We use the MMLU dataset (Hendrycks et al., 2020), which contains 57,000 questions spanning 57 topics. We select 5 topics for evaluation: high school chemistry, high school psychology, microeconomics, world history, and computer science. For each topic, we use the questions in the validation set as the in-context examples and the questions in the test set as the target questions. We generate explanations for all 1321 questions in the test set.

Text Generation We use the Google Natural Questions (NQ) dataset (Kwiatkowski et al., 2019) for text generation. We randomly select 200 questions from the validation set and generate short answers using the target models. To apply LIME and Kernel SHAP, we follow prior work (Luss et al., 2024; Hackmann et al., 2024; Liu and Zhang, 2025; Paes et al., 2024) in using a scoring function $f_s : \mathcal{X} \rightarrow \mathbb{R}$ that maps the generated sequence to a scalar score, effectively framing the text generation task as a regression problem. In our experiments, we use all-MiniLM-L6-v2 (Wang et al., 2020) from the Sentence-Transformers library (Reimers and Gurevych, 2019) as the scoring function. This pre-trained sentence transformer encodes each gen-

Table 2: Cost Reduction Ratios (CRR) achieved by using the proxy explanation framework to explain expensive LLMs with LIME and Kernel SHAP. Here, CRR_{mean} and CRR_{max} denote the average and maximum CRR obtained from screened budget-friendly models with API access. CRR_{local} is computed similarly to CRR_{max} but assumes all budget-friendly models are run locally at zero API cost. The $proxy_{\text{max}}$ row indicates the budget-friendly model that achieves CRR_{max} for each configuration; for MMLU, the reported $proxy_{\text{max}}$ is the most frequently selected proxy across the five subjects. Q denotes the Qwen 2.5 family.

Target Model		LIME			Kernel SHAP		
		SST	MMLU	NQ	SST	MMLU	NQ
GPT-4o	CRR_{mean}	8.74	3.41	10.14	8.90	3.41	12.12
	CRR_{max}	10.33	4.84	12.35	10.33	4.84	14.70
	CRR_{local}	14.17	5.62	25.32	14.17	5.62	27.78
	$proxy_{\text{max}}$	Q 7B	Q 7B	Q 0.5B	Q 7B	Q 7B	Q 7B
GPT-4o mini	CRR_{mean}	2.50	1.83	5.16	1.97	1.96	4.74
	CRR_{max}	3.08	2.88	9.52	3.10	3.19	10.42
	CRR_{local}	13.15	4.98	11.70	14.44	5.78	24.39
	$proxy_{\text{max}}$	Q 3B	Q 3B	Q 0.5B	Q 3B	Q 1.5B	Q 0.5B
DeepSeek V3	CRR_{mean}	3.06	2.15	4.82	3.88	2.27	5.37
	CRR_{max}	4.60	3.05	9.26	6.33	3.16	12.35
	CRR_{local}	13.31	5.32	15.15	13.64	6.10	15.15
	$proxy_{\text{max}}$	Q 3B	Q 1.5B	Q 0.5B	Q 1.5B	Q 1.5B	Q 1.5B
Qwen 2.5 14B	CRR_{mean}	2.39	1.82	4.47	1.85	1.90	4.88
	CRR_{max}	2.90	2.99	9.22	2.89	3.20	9.43
	CRR_{local}	17.13	5.64	32.26	17.13	6.10	32.26
	$proxy_{\text{max}}$	Q 3B	Q 1.5B	Q 0.5B	Q 3B	Q 1.5B	Q 0.5B
Qwen 2.5 32B	CRR_{mean}	3.18	2.06	5.16	3.19	2.16	5.19
	CRR_{max}	4.77	3.15	9.01	4.77	3.05	9.01
	CRR_{local}	15.24	5.30	17.86	15.24	5.31	17.86
	$proxy_{\text{max}}$	Q 3B	Q 1.5B	Q 1.5B	Q 3B	Q 1.5B	Q 1.5B
Qwen 2.5 72B	CRR_{mean}	5.10	2.47	6.75	5.05	2.76	7.45
	CRR_{max}	7.04	3.40	9.43	6.91	3.66	11.63
	CRR_{local}	16.25	6.07	17.09	16.25	6.31	24.39
	$proxy_{\text{max}}$	Q 3B	Q 7B	Q 0.5B	Q 3B	Q 7B	Q 1.5B
Llama 3.1 70B	CRR_{mean}	5.32	2.92	5.43	6.14	2.93	6.87
	CRR_{max}	6.74	3.96	6.62	8.02	3.96	10.42
	CRR_{local}	10.33	5.77	14.18	17.13	5.77	21.74
	$proxy_{\text{max}}$	Q 1.5B	Q 7B	Q 7B	Q 3B	Q 7B	Q 1.5B

Table 3: Screening recall, precision, and F1-score of the Proxy Explanation Framework.

Method	LIME			Kernel SHAP		
	SST	MMLU	NQ	SST	MMLU	NQ
Precision (%)	100.0	99.4	94.1	100.0	100.0	100.0
Recall (%)	80.2	77.6	76.1	96.3	97.2	96.2
F1-score (%)	89.0	87.2	84.2	98.1	98.5	98.0

erated answer into a semantic embedding vector, and we use the cosine similarity between the sample outputs and target outputs as the final scalar score.

4.2 Fidelity Metrics

LIME and Kernel SHAP construct a local surrogate model to approximate the target model’s behavior. Following Balagopalan et al. (2022); Yeh et al. (2019); Ismail et al. (2021), given a target

model f , an input x , a surrogate explanation model g , a neighborhood distribution $D(x)$, and a performance metric L (e.g., accuracy, AUROC, or mean squared error (MSE)), the (in)fidelity is defined as: $\mathbb{E}_{z \sim D(x)} L(f(z), g(z))$. In our experiments, we use **accuracy** as the performance metric L .

4.3 Evaluation Results

4.3.1 RQ1: Cost Reduction of Explaining Expensive LLMs

We use Cost Reduction Ratio (CRR) to measure the cost reduction achieved by our proxy explanation framework compared to directly generating explanations from expensive LLMs. Specifically, when explaining an expensive LLM f with a budget-friendly model f' on input set \mathbb{D} that passes the

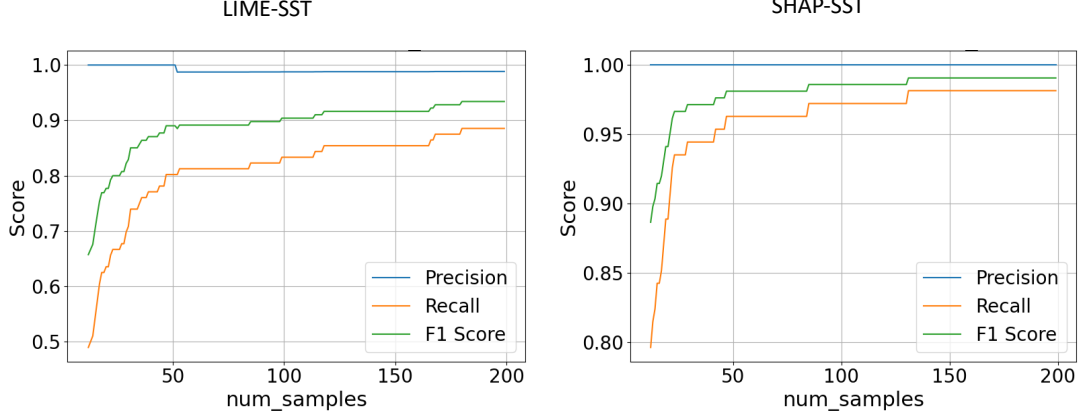


Figure 3: Impact of maximum sample size N on task-level screening results of proxy explanations on the SST dataset.

task-level screening step, we define the CRR as:

$$\text{CRR} = \frac{C_{\text{oracle}}}{C_{\text{proxy}} + C_{\text{fallback}} + C_{\text{screen}}}$$

where

$$\begin{aligned} C_{\text{oracle}} &= \sum_{\mathbf{x} \in \mathbb{D}} \text{Cost}(f, \mathbf{x}), \\ C_{\text{proxy}} &= \sum_{\mathbf{x} \in \mathbb{D}} \text{Cost}(f', \mathbf{x}) \cdot s_{\text{inst}}(\mathbf{x}; f, f'), \\ C_{\text{fallback}} &= \sum_{\mathbf{x} \in \mathbb{D}} \text{Cost}(f, \mathbf{x}) \cdot (1 - s_{\text{inst}}(\mathbf{x}; f, f')), \\ C_{\text{screen}} &= \text{Cost}_{\text{screen}}(f, f', \mathbb{D}), \end{aligned}$$

where $\text{Cost}(f, \mathbf{x})$ denotes the cost of generating explanations for model f , $s_{\text{inst}}(\mathbf{x}; f, f')$ is the instance-level screening function defined in Section 3, and $\text{Cost}_{\text{screen}}(f, f', \mathbb{D})$ is the cost of performing task-level screening on dataset \mathbb{D} . Here, we split the models into two groups based on their costs: all models that can be run locally on a single consumer-grade GPU are considered budget-friendly models, while the rest are classified as target expensive models.

Table 2 shows the CRR achieved by using our proxy explanation framework to explain expensive LLMs with LIME and Kernel SHAP. We can see that for each expensive model, the use of a budget-friendly proxy model significantly reduces the cost of generating explanations. Especially for the most expensive model GPT-4o, using proxy explanations from budget-friendly models can save on average 90.5% of the cost across all these tasks. The *proxy_{max}* row in Table 2 further lists the specific budget-friendly model that achieves CRR_{max} for each target model, explanation method, and dataset. A clear pattern emerges: Qwen 2.5 models with small parameter counts consistently serve as the

best proxies across target–task combinations, suggesting that a small set of budget-friendly models is often sufficient to cover a wide range of expensive targets.

4.3.2 RQ2: Reliability of Screening Step

Our task-level screening verifies whether proxy explanations from a budget-friendly model f' can, on the input set \mathbb{D} , achieve fidelity comparable to the oracle explanations generated directly from f . For each task, we validate the reliability of the screening step by checking if the screening results align with the actual fidelity of proxy explanations. Since the screening decision is a binary classification problem, we assess its reliability using standard classification metrics: Precision, Recall, and F1-score.

Table 3 shows that our task-level screening step achieves 98.9% precision on average, which means that the screening is sufficient to ensure the fidelity of proxy explanations. For the rare false positives, the realized proxy fidelity still exceeds 89% of the oracle on average, suggesting that even misclassifications remain reasonably faithful. On the other hand, although recall is lower, the results of RQ1 demonstrate that for each expensive model there exists at least one budget-friendly model that passes the screening. Given that budget-friendly models are inexpensive to run, users can screen multiple candidates in parallel to reliably identify a suitable proxy model.

Hyperparameter Sensitivity We study the impact of hyperparameters used in our experiments. We primarily investigate the impact of the maximum sample size on the effectiveness of task-level

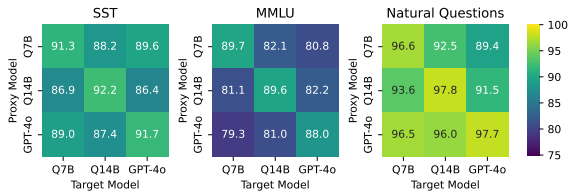


Figure 4: Accuracy of proxy LIME explanations on SST, MMLU, and Natural Questions datasets.

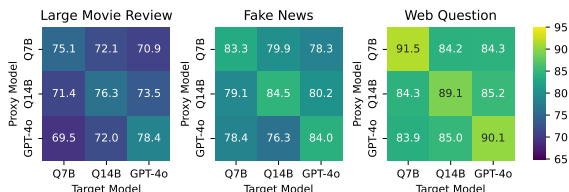


Figure 5: Accuracy of proxy LIME explanations on Large Movie Review, Fake News, and Web Question datasets.

screening. Figure 3 shows the results of task-level screening on the SST dataset with different maximum sample sizes N . We observe that as N increases, the recall of task-level screening also increases, while the precision remains consistently high.

4.3.3 RQ3: Generalizability of Proxy Explanations

To validate whether the cross-model explanation transferability holds across different tasks and datasets, we conduct experiments on the datasets described in Section 4.1 and three additional datasets: Large Movie Review (Maas et al., 2011), Fake News (Pérez-Rosas et al., 2018), and Web Questions (Berant et al., 2013) for text generation. Overall, we observe that the findings from the three main datasets generally hold across these additional datasets, demonstrating the generalizability of our proxy explanation framework. Due to space limitations, we only show the results of cross-model proxy explanation fidelity between GPT-4o, Qwen2.5-7B, and Qwen2.5-14B on the six tasks in Figure 4 and 5. For GPT-4o, Qwen2.5-7B and Qwen2.5-14B can both achieve over 90% fidelity compared to the oracle explanations.

For more detailed results and analysis, please refer to Appendix E.

5 Actionable Utility Evaluation

Having established the statistical fidelity of proxy explanations in the previous section, we now eval-

uate the **actionable utility** of our framework in real-world optimization scenarios. We focus on **In-Context Learning (ICL)** settings, where the quality of the input prompt directly dictates model performance. In this context, explanations serve not only as passive observations, but also as active signals to diagnose redundancy or identify malicious patterns.

Specifically, we use proxy explanations generated from budget-friendly models that have passed the screening step, to guide two distinct optimization tasks, and compare their effectiveness against baselines including using oracle explanations and other state-of-the-art methods. We demonstrate this utility across two distinct tasks: (1) **Prompt Compression (Efficiency)**; and (2) **Poisoned Example Removal (Safety)**.

5.1 Task 1: Prompt Compression

Prompt compression aims to help users save costs by reducing the number of examples in the prompt while maintaining the model’s performance.

Experiment Setup We use explanations to compress the ICL examples when using GPT-4o to answer questions from five subjects from MMLU (Hendrycks et al., 2020), HelLaSwag (Zellers et al., 2019), GSM8K (Cobbe et al., 2021), and PIQA (Bisk et al., 2019). We compress the prompt by removing the least important examples based on KSHAP explanations. Concretely, we define the prompt compression task as follows: Given a set of examples S , an explanation g that attributes the importance of each example, we iteratively remove the least important examples based on g . The goal is to remove as many examples as possible while ensuring that GPT-4o’s performance stays above a certain threshold τ compared to using all examples (we set $\tau = 0.9$). We use the compression ratio as the metric, which is defined as $\text{CompressionRatio}(g) = 1 - \frac{|S_g^\tau|}{|S|}$, where S_g^τ is the set of examples retained after applying the explanation g and ensuring the model’s performance remains above the threshold τ . A higher compression ratio indicates a more effective explanation. We verify if the proxy explanations from a budget-friendly model of Qwen 2.5 series can achieve similar performance as oracle explanations from GPT-4o. Additionally, we also compare the performance of proxy explanations with a random deletion baseline, and two state-of-the-art prompt compression methods, AttnComp (Zhao et al., 2025) and LLM-

Table 4: Comparison of compression ratios (%) using oracle explanations, proxy explanations, random deletions and other baselines for in-context learning prompt compression across various tasks.

Task	MMLU-Chem.	MMLU-CS	MMLU-Micro.	MMLU-Psy.	MMLU-WH	HellaSwag	GSM8K	PIQA
Random	29.0	35.6	59.8	61.0	43.4	58.8	25.3	54.3
AttnComp (w/ proxy)	34.5	39.1	63.2	66.5	47.1	64.3	30.2	60.2
LLMLingua	38.7	38.3	62.5	66.1	46.3	62.7	28.9	58.7
Proxy Exp.	41.0	43.0	67.6	69.8	52.0	70.1	35.5	64.5
Oracle Exp.	49.2	50.2	72.8	72.8	57.0	75.5	37.2	69.2

Table 5: Comparison of accuracy (%) of GPT-4o after using different methods to remove poisoned examples.

Method	SST	HellaSwag	PIQA
Random deletion	87.1	88.4	79.6
Proxy Exp.	94.0	93.5	90.7
Oracle Exp.	94.2	93.7	91.5

Lingua (Jiang et al., 2023). Since AttnComp is a white-box method, we apply it on the same proxy model used by our method.

For each dataset, we repeat the experiment 15 times with different ICL examples and test questions.

Evaluation Results Table 4 shows the results. Proxy explanations achieve performance comparable to the oracle explanations from GPT-4o, reaching an average of 91.3% of the oracle’s performance. Moreover, they outperform random deletions and two state-of-the-art prompt compression methods.

5.2 Task 2: Poisoned Examples Removal

While ICL is useful, poisoned examples can lead to suboptimal performance (Ranjan et al., 2023). Outlier removal focuses on identifying and removing examples that may negatively impact the model’s performance, thereby improving the overall quality of the prompt.

Experiment Setup We use GPT-4o to perform classification tasks on SST-2 (Socher et al., 2013), HellaSwag (Zellers et al., 2019), and PIQA (Bisk et al., 2019) as our target tasks. We add poisoning examples to the original dataset, until the accuracy of GPT-4o drops to lower than 80%, and then use explanations to identify and remove these outliers. We follow the explanation to remove all negatively attributed examples, and evaluate the model’s performance after removal. We compare the performance using oracle explanations from GPT-4o and proxy explanations generated by our

methods, along with a random deletion baseline.

Evaluation Results Table 5 shows the results. After removing the poisoned examples based on explanations, the accuracy of GPT-4o recovers significantly, and proxy explanations achieve comparable performance to oracle explanations, both significantly outperforming random deletion.

6 Conclusion

In this paper, we introduced a screen-and-apply proxy explanation framework that leverages budget-friendly models to generate proxy explanations for LLMs, reducing the cost of local model-agnostic explanations and enabling their practical use. We demonstrated the effectiveness of our approach through extensive experiments across various tasks and models. The results indicate that our proxy explanations maintain a high level of fidelity compared to oracle explanations while significantly reducing the cost by 90.5%. We also show that our proxy explanations can effectively guide the optimization of expensive LLMs in in-context learning scenarios.

Limitations

Our work focuses on perturbation-based feature attribution for black-box LLMs. While our *Screen-and-Apply* mechanism ensures reliability, we acknowledge that in scenarios requiring extreme reasoning capabilities (e.g., complex symbolic logic), the alignment between small proxies and large oracles may weaken. In such cases, our framework prioritizes safety by falling back to the oracle, which guarantees fidelity but may reduce the magnitude of cost savings. To mitigate this, a potential direction is to align proxy models with oracles through lightweight fine-tuning. We leave this exploration to future work.

Ethical Considerations

While our framework aims to democratize LLM interpretability and enhance model transparency, we acknowledge the dual-use nature of local explanations. Such methods could potentially be misused to facilitate adversarial attacks or generate misleading interpretations of model behavior. We strongly encourage responsible application of our framework and dataset, and emphasize the necessity of robust safeguards when deploying explanation tools in sensitive or high-stakes domains.

Acknowledgments

This work was sponsored by the National Natural Science Foundation of China (NSFC) under Grant No. W2411051.

References

- Aparna Balagopalan, Haoran Zhang, Kimia Hamidieh, Thomas Hartvigsen, Frank Rudzicz, and Marzyeh Ghassemi. 2022. The road to explainability is paved with bias: Measuring the fairness of explanations. In *Proceedings of the 2022 ACM Conference on Fairness, Accountability, and Transparency*, pages 1194–1206.
- Jonathan Berant, Andrew Chou, Roy Frostig, and Percy Liang. 2013. [Semantic parsing on Freebase from question-answer pairs](#). In *Proceedings of the 2013 Conference on Empirical Methods in Natural Language Processing*, pages 1533–1544, Seattle, Washington, USA. Association for Computational Linguistics.
- Yonatan Bisk, Rowan Zellers, Ronan Le Bras, Jianfeng Gao, and Yejin Choi. 2019. [Piqa: Reasoning about physical commonsense in natural language](#). *Preprint*, arXiv:1911.11641.
- Jianbo Chen, Le Song, Martin Wainwright, and Michael Jordan. 2018. [Learning to explain: An information-theoretic perspective on model interpretation](#). In *Proceedings of the 35th International Conference on Machine Learning*, volume 80 of *Proceedings of Machine Learning Research*, pages 883–892. PMLR.
- Yu-Neng Chuang, Guanchu Wang, Fan Yang, Zirui Liu, Xuanting Cai, Mengnan Du, and Xia Hu. 2023a. [Efficient xai techniques: A taxonomic survey](#). *Preprint*, arXiv:2302.03225.
- Yu-Neng Chuang, Guanchu Wang, Fan Yang, Quan Zhou, Pushkar Tripathi, Xuanting Cai, and Xia Hu. 2023b. [Cortx: Contrastive framework for real-time explanation](#). *Preprint*, arXiv:2303.02794.
- Karl Cobbe, Vineet Kosaraju, Mohammad Bavarian, Mark Chen, Heewoo Jun, Lukasz Kaiser, Matthias Plappert, Jerry Tworek, Jacob Hilton, Reiichiro Nakano, Christopher Hesse, and John Schulman. 2021. [Training verifiers to solve math word problems](#). *Preprint*, arXiv:2110.14168.
- Ian Covert, Chanwoo Kim, Su-In Lee, James Zou, and Tatsunori Hashimoto. 2024. [Stochastic amortization: A unified approach to accelerate feature and data attribution](#). In *Advances in Neural Information Processing Systems*, volume 37, page 4374–4423. Curran Associates, Inc.
- David Dandolo, Chiara Masiero, Mattia Carletti, Davide Dalle Pezze, and Gian Antonio Susto. 2023. [Acme—accelerated model-agnostic explanations: Fast whitening of the machine-learning black box](#). *Expert Systems with Applications*, 214:119115.
- DeepSeek-AI, Aixin Liu, Bei Feng, Bing Xue, Bingxuan Wang, Bochao Wu, Chengda Lu, Chenggang Zhao, Chengqi Deng, Chenyu Zhang, Chong Ruan, Damai Dai, Daya Guo, Dejian Yang, Deli Chen, Dongjie Ji, Erhang Li, Fangyun Lin, Fucong Dai, and 181 others. 2025. [Deepseek-v3 technical report](#). *Preprint*, arXiv:2412.19437.
- Rudresh Dwivedi, Devam Dave, Het Naik, Smiti Singhal, Rana Omer, Pankesh Patel, Bin Qian, Zhenyu Wen, Tejal Shah, and Graham Morgan. 2023. [Explainable ai \(xai\): Core ideas, techniques, and solutions](#). *ACM Computing Surveys*, 55(9):1–33.
- James Enouen, Hootan Nakhost, Sayna Ebrahimi, Serkan Arik, Yan Liu, and Tomas Pfister. 2024. [TextGenSHAP: Scalable post-hoc explanations in text generation with long documents](#). In *Findings of the Association for Computational Linguistics: ACL 2024*, pages 13984–14011, Bangkok, Thailand. Association for Computational Linguistics.
- Gemini Team Google, Rohan Anil, Sebastian Borgeaud, Jean-Baptiste Alayrac, Jiahui Yu, Radu Soricut, Johan Schalkwyk, Andrew M. Dai, Anja Hauth, Katie Millican, David Silver, Melvin Johnson, Ioannis Antonoglou, Julian Schrittwieser, Amelia Glaese, Jilin Chen, Emily Pitler, Timothy Lillicrap, Angeliki Lazaridou, and 1332 others. 2025. [Gemini: A family of highly capable multimodal models](#). *Preprint*, arXiv:2312.11805.
- Aaron Grattafiori, Abhimanyu Dubey, Abhinav Jauhri, Abhinav Pandey, Abhishek Kadian, Ahmad Al-Dahle, Aiesha Letman, Akhil Mathur, Alan Schelten, Alex Vaughan, Amy Yang, Angela Fan, Anirudh Goyal, Anthony Hartshorn, Aobo Yang, Archi Mitra, Archie Sravankumar, Artem Korenev, Arthur Hinsvark, and 542 others. 2024. [The llama 3 herd of models](#). *Preprint*, arXiv:2407.21783.
- Stefan Hackmann, Haniyeh Mahmoudian, Mark Steadman, and Michael Schmidt. 2024. [Word importance explains how prompts affect language model outputs](#). *Preprint*, arXiv:2403.03028.
- Dan Hendrycks, Collin Burns, Steven Basart, Andy Zou, Mantas Mazeika, Dawn Song, and Jacob Steinhardt.

2020. Measuring massive multitask language understanding. *arXiv preprint arXiv:2009.03300*.
- Aya Abdelsalam Ismail, Hector Corrada Bravo, and Soheil Feizi. 2021. Improving deep learning interpretability by saliency guided training. *Advances in Neural Information Processing Systems*, 34:26726–26739.
- Neil Jethani, Mukund Sudarshan, Ian Connick Covert, Su-In Lee, and Rajesh Ranganath. 2022. **FastSHAP: Real-time shapley value estimation**. In *International Conference on Learning Representations*.
- Huiqiang Jiang, Qianhui Wu, Chin-Yew Lin, Yuqing Yang, and Lili Qiu. 2023. **Llmlingua: Compressing prompts for accelerated inference of large language models**. *Preprint*, arXiv:2310.05736.
- Liwei Jiang, Yuanjun Chai, Margaret Li, Mickel Liu, Raymond Fok, Nouha Dziri, Yulia Tsvetkov, Maarten Sap, Alon Albalak, and Yejin Choi. 2025. Artificial hivemind: The open-ended homogeneity of language models (and beyond). *arXiv preprint arXiv:2510.22954*.
- Martin Jullum, Annabelle Redelmeier, and Kjersti Aas. 2021. groupshapley: Efficient prediction explanation with shapley values for feature groups. *arXiv preprint arXiv:2106.12228*.
- Tom Kwiatkowski, Jennimaria Palomaki, Olivia Redfield, Michael Collins, Ankur Parikh, Chris Alberti, Danielle Epstein, Illia Polosukhin, Jacob Devlin, Kenton Lee, Kristina Toutanova, Llion Jones, Matthew Kelcey, Ming-Wei Chang, Andrew M. Dai, Jakob Uszkoreit, Quoc Le, and Slav Petrov. 2019. **Natural questions: A benchmark for question answering research**. *Transactions of the Association for Computational Linguistics*, 7:452–466.
- Sunbowen Lee, Juntong Zhou, Chang Ao, Kaige Li, Xinrun Du, Sirui He, Haihong Wu, Tianci Liu, Jiaheng Liu, Hamid Alinejad-Rokny, Min Yang, Yitao Liang, Zhoufutu Wen, and Shiwen Ni. 2025. **Quantification of large language model distillation**. (arXiv:2501.12619). ArXiv:2501.12619 [cs].
- Junhao Liu, Haonan Yu, Zhenyu Yan, and Xin Zhang. 2026a. **Focus-lime: Surgical interpretation of long-context large language models via proxy-based neighborhood selection**. *Preprint*, arXiv:2602.04607.
- Junhao Liu, Haonan Yu, and Xin Zhang. 2026b. **Beyond attribution: Unified concept-level explanations**. *Preprint*, arXiv:2410.12439.
- Junhao Liu and Xin Zhang. 2025. Rex: A framework for incorporating temporal information in model-agnostic local explanation techniques. In *Proceedings of the AAAI Conference on Artificial Intelligence*, volume 39, pages 18888–18896.
- Scott M. Lundberg and Su-In Lee. 2017. A unified approach to interpreting model predictions. In *Advances in Neural Information Processing Systems 30: Annual Conference on Neural Information Processing Systems 2017, December 4-9, 2017, Long Beach, CA, USA*, pages 4765–4774.
- Ronny Luss, Erik Miehling, and Amit Dhurandhar. 2024. Cell your model: Contrastive explanations for large language models. *arXiv preprint arXiv:2406.11785*.
- Andrew L. Maas, Raymond E. Daly, Peter T. Pham, Dan Huang, Andrew Y. Ng, and Christopher Potts. 2011. **Learning word vectors for sentiment analysis**. In *Proceedings of the 49th Annual Meeting of the Association for Computational Linguistics: Human Language Technologies*, pages 142–150, Portland, Oregon, USA. Association for Computational Linguistics.
- Manoj Kumar Mahto. 2024. Explainable artificial intelligence: Fundamentals, approaches, challenges, xai evaluation, and validation. In *Explainable Artificial Intelligence for Autonomous Vehicles*, pages 25–49. CRC Press.
- Rory Mitchell, Joshua Cooper, Eibe Frank, and Geoffrey Holmes. 2022. **Sampling permutations for shapley value estimation**. *Preprint*, arXiv:2104.12199.
- OpenAI, Josh Achiam, Steven Adler, Sandhini Agarwal, Lama Ahmad, Ilge Akkaya, Florencia Leoni Aleman, Diogo Almeida, Janko Altenschmidt, Sam Altman, Shyamal Anadkat, Red Avila, Igor Babuschkin, Suchir Balaji, Valerie Balcom, Paul Baltescu, Haiming Bao, Mohammad Bavarian, Jeff Belgum, and 262 others. 2024. **Gpt-4 technical report**. *Preprint*, arXiv:2303.08774.
- Lucas Monteiro Paes, Dennis Wei, Hyo Jin Do, Hendrik Strobelt, Ronny Luss, Amit Dhurandhar, Manish Naregreddy, Karthikeyan Natesan Ramamurthy, Prasanna Sattigeri, Werner Geyer, and Soumya Ghosh. 2024. **Multi-level explanations for generative language models**. *Preprint*, arXiv:2403.14459.
- Verónica Pérez-Rosas, Bennett Kleinberg, Alexandra Lefevre, and Rada Mihalcea. 2018. **Automatic detection of fake news**. In *Proceedings of the 27th International Conference on Computational Linguistics*, pages 3391–3401, Santa Fe, New Mexico, USA. Association for Computational Linguistics.
- Sudhanshu Ranjan, Chung-En Sun, Linbo Liu, and Tsui-Wei Weng. 2023. **Fooling GPT with adversarial in-context examples for text classification**. In *RO-FoMo: Robustness of Few-shot and Zero-shot Learning in Large Foundation Models*.
- Nils Reimers and Iryna Gurevych. 2019. **Sentence-bert: Sentence embeddings using siamese bert-networks**. In *Proceedings of the 2019 Conference on Empirical Methods in Natural Language Processing*. Association for Computational Linguistics.
- Marco Túlio Ribeiro, Sameer Singh, and Carlos Guestrin. 2016. “why should I trust you?”: Explaining the predictions of any classifier. In *Proceedings of the 22nd ACM SIGKDD International Conference*

- on *Knowledge Discovery and Data Mining, San Francisco, CA, USA, August 13-17, 2016*, pages 1135–1144. ACM.
- Thomas Rojat, Raphaël Puget, David Filliat, Javier Del Ser, Rodolphe Gelin, and Natalia Díaz-Rodríguez. 2021. Explainable artificial intelligence (xai) on timeseries data: A survey. *arXiv preprint arXiv:2104.00950*.
- Taylor Shin, Yasaman Razeghi, Robert L. Logan IV, Eric Wallace, and Sameer Singh. 2020. AutoPrompt: Eliciting knowledge from language models with automatically generated prompts. In *Empirical Methods in Natural Language Processing (EMNLP)*.
- Richard Socher, Alex Perelygin, Jean Wu, Jason Chuang, Christopher D Manning, Andrew Y Ng, and Christopher Potts. 2013. Recursive deep models for semantic compositionality over a sentiment treebank. In *Proceedings of the 2013 conference on empirical methods in natural language processing*, pages 1631–1642.
- Ian Tenney, Ryan Mullins, Bin Du, Shree Pandya, Min-suk Kahng, and Lucas Dixon. 2024. Interactive prompt debugging with sequence salience. *arXiv preprint arXiv:2404.07498*.
- Guanchu Wang, Yu-Neng Chuang, Mengnan Du, Fan Yang, Quan Zhou, Pushkar Tripathi, Xuanting Cai, and Xia Hu. 2022. [Accelerating shapley explanation via contributive cooperator selection](#). In *Proceedings of the 39th International Conference on Machine Learning*, volume 162 of *Proceedings of Machine Learning Research*, pages 22576–22590. PMLR.
- Wenhui Wang, Furu Wei, Li Dong, Hangbo Bao, Nan Yang, and Ming Zhou. 2020. [Minilm: Deep self-attention distillation for task-agnostic compression of pre-trained transformers](#). *Preprint*, arXiv:2002.10957.
- Dustin Wright, Sarah Masud, Jared Moore, Srishti Yadav, Maria Antoniak, Chan Young Park, and Isabelle Augenstein. 2025. [Epistemic diversity and knowledge collapse in large language models](#). (arXiv:2510.04226). ArXiv:2510.04226 [cs].
- Qwen: An Yang, Baosong Yang, Beichen Zhang, Binyuan Hui, Bo Zheng, Bowen Yu, Chengyuan Li, Dayiheng Liu, Fei Huang, Haoran Wei, Huan Lin, Jian Yang, Jianhong Tu, Jianwei Zhang, Jianxin Yang, Jiayi Yang, Jingren Zhou, Junyang Lin, Kai Dang, and 23 others. 2025. [Qwen2.5 technical report](#). *Preprint*, arXiv:2412.15115.
- Chih-Kuan Yeh, Cheng-Yu Hsieh, Arun Suggala, David I Inouye, and Pradeep K Ravikumar. 2019. On the (in) fidelity and sensitivity of explanations. *Advances in Neural Information Processing Systems*, 32.
- Jinsung Yoon, James Jordon, and Mihaela van der Schaar. 2019. [INVASE: Instance-wise variable selection using neural networks](#). In *International Conference on Learning Representations*.
- Haonan Yu, Junhao Liu, and Xin Zhang. 2026. [Manchors: Memorization-based acceleration of anchors via rule reuse and transformation](#). *Preprint*, arXiv:2502.11068.
- Rowan Zellers, Ari Holtzman, Yonatan Bisk, Ali Farhadi, and Yejin Choi. 2019. [Hellaswag: Can a machine really finish your sentence?](#) *Preprint*, arXiv:1905.07830.
- Yu Zhang, Peter Tiño, Aleš Leonardis, and Ke Tang. 2021. [A survey on neural network interpretability](#). *IEEE Transactions on Emerging Topics in Computational Intelligence*, 5(5):726–742. ArXiv:2012.14261 [cs].
- Yunlong Zhao, Haoran Wu, and Bo Xu. 2025. Leveraging attention to effectively compress prompts for long-context llms. In *Proceedings of the AAAI Conference on Artificial Intelligence*, volume 39, pages 26048–26056.
- Yilun Zhou, Caiming Xiong, Silvio Savarese, and Chien-Sheng Wu. 2024. Shared imagination: Llms hallucinate alike. *arXiv preprint arXiv:2407.16604*.

A The Use of Large Language Models

We use LLMs to refine and polish human writing, and find related work with DeepResearch. We do not use LLMs to generate the main content or ideas of this paper.

B Datasets

To reduce the cost of future research on black-box explanation generation for LLMs, improve accessibility, and facilitate reproducibility, we have open-sourced the datasets used in our experiments. In particular, since querying LLMs for perturbed samples is the most computationally expensive part of the process, we provide the model outputs for all perturbed samples used in our experiments. For LIME, perturbations are generated following the original implementation,² and for Kernel SHAP, we use the implementation provided by the Captum library.³ We generate 1000 perturbed samples for each input instance explained.

As mentioned in Section 1, the datasets cover three tasks: sentiment analysis, multiple-choice question answering, and text generation. For each perturbed sample, we collect the model output logits of the first predicted token. We release the model outputs for each perturbed sample of these questions for reproducibility. As we create the datasets with public datasets and publicly accessible models, there are no ethical or legal issues involved in releasing these datasets.

C Proxy Explanation Framework Details

As most budget-friendly models can be run locally, we can perform the task-level screening for multiple budget-friendly models at the same time, as shown in Algorithm 1.

To avoid redundant oracle queries, we introduce a shared buffer that stores each input and the corresponding output from the target model f . Formally, we construct

$$\mathcal{B} = \{(x, f(x)) : x \in \mathbb{D}\}.$$

This buffer is built once and reused across all candidate proxy models $\{f'_1, \dots, f'_m\}$.

Each time we calculate fidelity, if the output of x and its neighborhood are already in the buffer \mathcal{B} , we can directly use the cached values. This avoids redundant calls to the target model f and speeds up the screening process.

²<https://github.com/marcotcr/lime>

³https://captum.ai/api/kernel_shap.html

D Experimental Setup Details

D.1 Models

We run Qwen2.5 and Llama3.1 models locally on a machine with total 576 GiB VRAM, while GPT-4o and DeepSeekV3 models are accessed via their official APIs. When locally running the models, we use the default version without additional quantization or distillation.

D.2 Sentiment Analysis

We perform sentiment analysis using LLMs in a zero-shot setting, where the model is prompted to classify the sentiment of a given sentence as either "positive" or "negative." The sentiment classification task is defined in the system prompt, while the specific sentence to be classified is provided in the user input. The following prompt templates are used:

system_prompt:

```
From now on, you should act as a sentiment analysis neural network. You should classify the sentiment of a sentence into positive or negative. The input sentence may be empty. In each task, you will be given the sentences to be classified, which end with #####, and then you should reply the sentiment of the sentence by positive or negative.
```

user_prompt:

```
Perform the following task, your answer should only be positive or negative:
Sentence:
{input_sentence}
#####
Sentiment:
```

To obtain the class probabilities, we use the probabilities of the first output token. Specifically, we extract the logits corresponding to the tokens

"positive" and "negative" from the model output and apply the softmax function to compute the probability distribution over the two classes. For local models, we directly obtain the logits and compute the softmax. For GPT-4o and DeepSeekV3, we use their official APIs with the temperature set to 1, retrieve the log probabilities of the target tokens, and then apply the softmax function to obtain normalized probabilities.

D.3 Multiple-Choice Question Answering

We perform multiple-choice question answering using LLMs with few-shot prompting, where the model is provided with all examples from the development set using the in-context learning template recommended by OpenAI,⁴ as illustrated in Figure 6. We follow the official instructions provided in OpenAI Evals.⁵

The prompt template is as follows:

```

System: The following are
multiple choice questions (with
answers) about {subject}.
User: {example question 1}
Assistant: {example answer 1}
:
User: {question to be answered}

```

To obtain the class probabilities, we use similar logit extraction methods as in the sentiment analysis task. Specifically, we extract the logits corresponding to the tokens "A", "B", "C", and "D" from the model output and apply the softmax function to compute the probability distribution over the four classes.

D.4 Text Generation

As mentioned in Section 4.1, we treat this task as a regression problem by using a scoring function to evaluate the generated text. When generating text with LLMs, we set the temperature to 1e-5 or set `do_sample = False` to ensure deterministic outputs. We limit the maximum number of generated tokens to 20 and prompt the model to generate short answers, in line with the short-answer format of the Natural Questions dataset. Specifically, we use the following prompt template:

⁴<https://platform.openai.com/docs/guides/prompt-engineering/six-strategies-for-getting-better-results#tactic-provide-examples>

⁵<https://github.com/openai/evals/blob/main/examples/mmlu.ipynb>

```

[
{"role": "system", "content":
  "You are a helpful assistant.
  Answer the question briefly,
  within 10 words. You will be
  penalized for overly long answers."
},
{"role": "user",
"content": "{Question}"}
]

```

E RQ3: Generalizability of Proxy Explanation Details

In this section, we further analyze the evaluation results.

E.1 Sentiment Analysis

We have presented the fidelity of proxy LIME and Kernel SHAP explanations after instance-level screening in Figure 7.

E.2 Multiple-Choice Question Answering

We have provided overall fidelity results in Figure 8.

We also provide the explanation fidelity results on each subject in Figure 9 and Figure 10. We can see that our instance-level screening method can effectively improve the fidelity of proxy explanations. Additionally, we also provide the detailed results with 95% confidence intervals in Table 6, 7, 8, 9, 10, 11, 12, 13, 14, 15, 16, 17, 18, 19, 20, 21, 22, 23, 24, and 25.

Another notable observation is that the fidelity of oracle explanations also differs across subjects. For high school microeconomics, high school psychology, and high school world history, the oracle LIME explanations generated by the model all achieve a fidelity higher than 90%, while for high school computer science and high school chemistry, the fidelity is relatively lower. The subjects with higher fidelity are all related to social sciences, while the subjects with lower fidelity are all related to natural sciences. This may be because natural science questions often demand precise, computation-intensive reasoning (e.g., numerical calculations or formula application), where even small differences in model capability can lead to divergent local decision boundaries and thus lower surrogate fidelity. In contrast, social science questions rely more on broad textual comprehension, where different models tend to exhibit more homogeneous behavior, resulting in higher fidelity.

Tactic: Provide examples

Providing general instructions that apply to all examples is generally more efficient than demonstrating all permutations of a task by example, but in some cases providing examples may be easier. For example, if you intend for the model to copy a particular style of responding to user queries which is difficult to describe explicitly. This is known as "few-shot" prompting.

SYSTEM	Answer in a consistent style.
USER	Teach me about patience.
ASSISTANT	The river that carves the deepest valley flows from a modest spring; the grandest symphony originates from a single note; the most intricate tapestry begins with a solitary thread.
USER	Teach me about the ocean.

Figure 6: The recommended few-shot template provided by OpenAI.

F Licenses of Used Artifacts

We list the licenses of all the major artifacts used in our work as follows:

- LIME: MIT License
- SHAP: MIT License
- MMLU dataset: MIT License
- SST-2 dataset: CC0: Public Domain
- Natural Questions dataset: Apache License 2.0
- Qwen2.5 models: Apache License 2.0
- Llama3.1 models: llama 3.1 license
- DeepSeekV3 model: MIT License
- Large Movie Review Dataset: CC0 Public Domain
- Web Questions: CC0 Public Domain
- HellaSwag: CC0 Public Domain
- GSM8K: MIT License

We use all these artifacts in a manner consistent with their intended use and in compliance with their respective licenses.

G Resource Usage

We conducted all experiments on servers with GPUs that each have 80GB VRAM. The total computation time is around 3,000 GPU hours. The total cost of using GPT-4o and DeepSeekV3 APIs is around 20,000 USD.

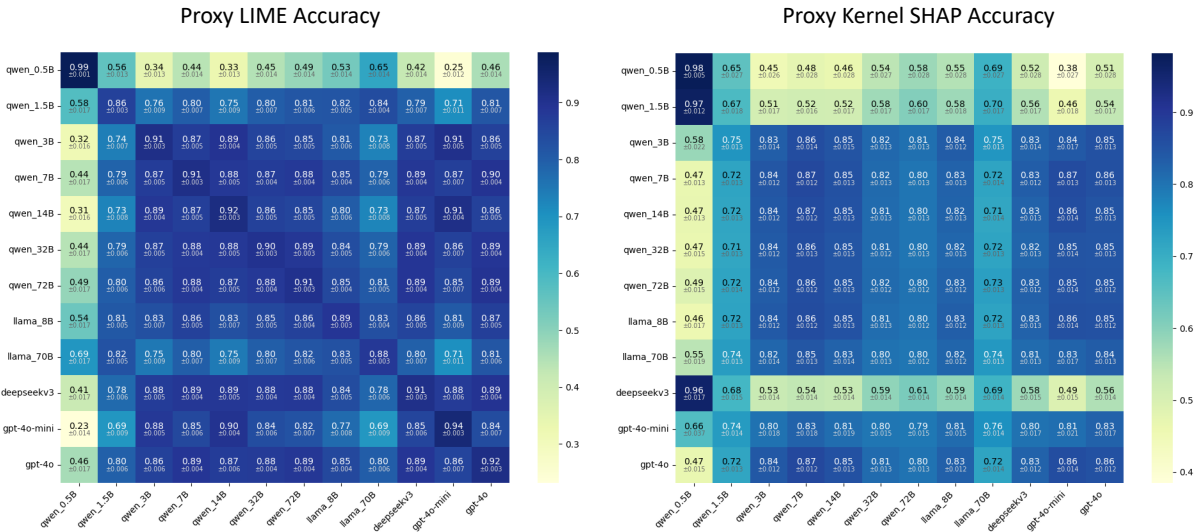


Figure 7: Accuracy of proxy explanations on the text classification task: each cell shows how well explanations generated by the model on the **y-axis** serve as surrogates for predicting the behavior of the model on the **x-axis**. The smaller text below each value indicates the 95% confidence interval. The heatmap on the right shows results after filtering out examples where the budget-friendly and expensive models produce different predictions for the input.

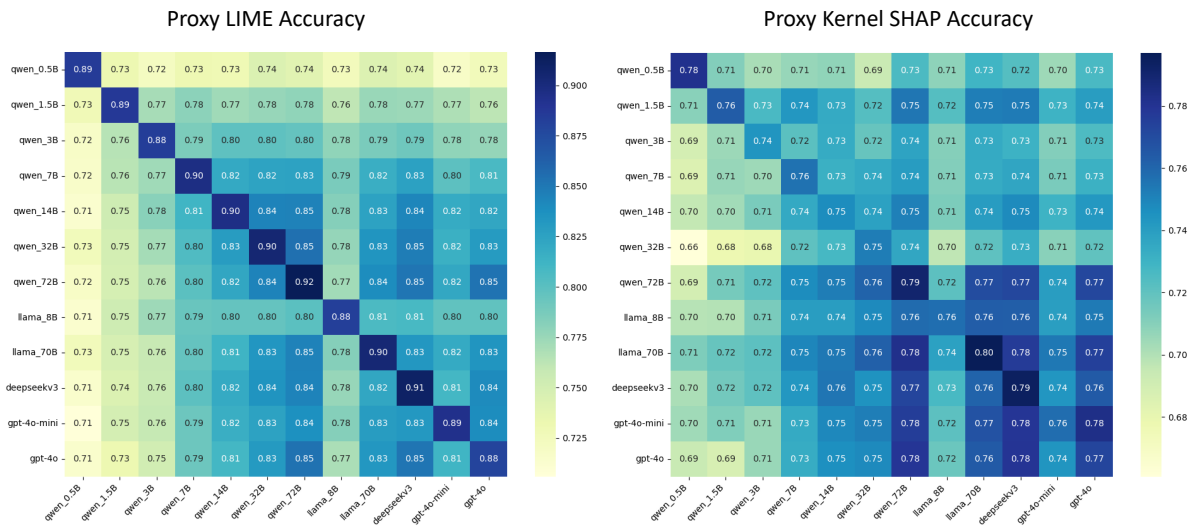


Figure 8: Accuracy of LIME proxy explanations on the multiple-choice question answering task. Each cell shows how well explanations generated by the model on the **y-axis** serve as surrogates for predicting the behavior of the model on the **x-axis**. The heatmap on the right shows results after filtering out examples where the budget-friendly and expensive models produce different predictions for the input.

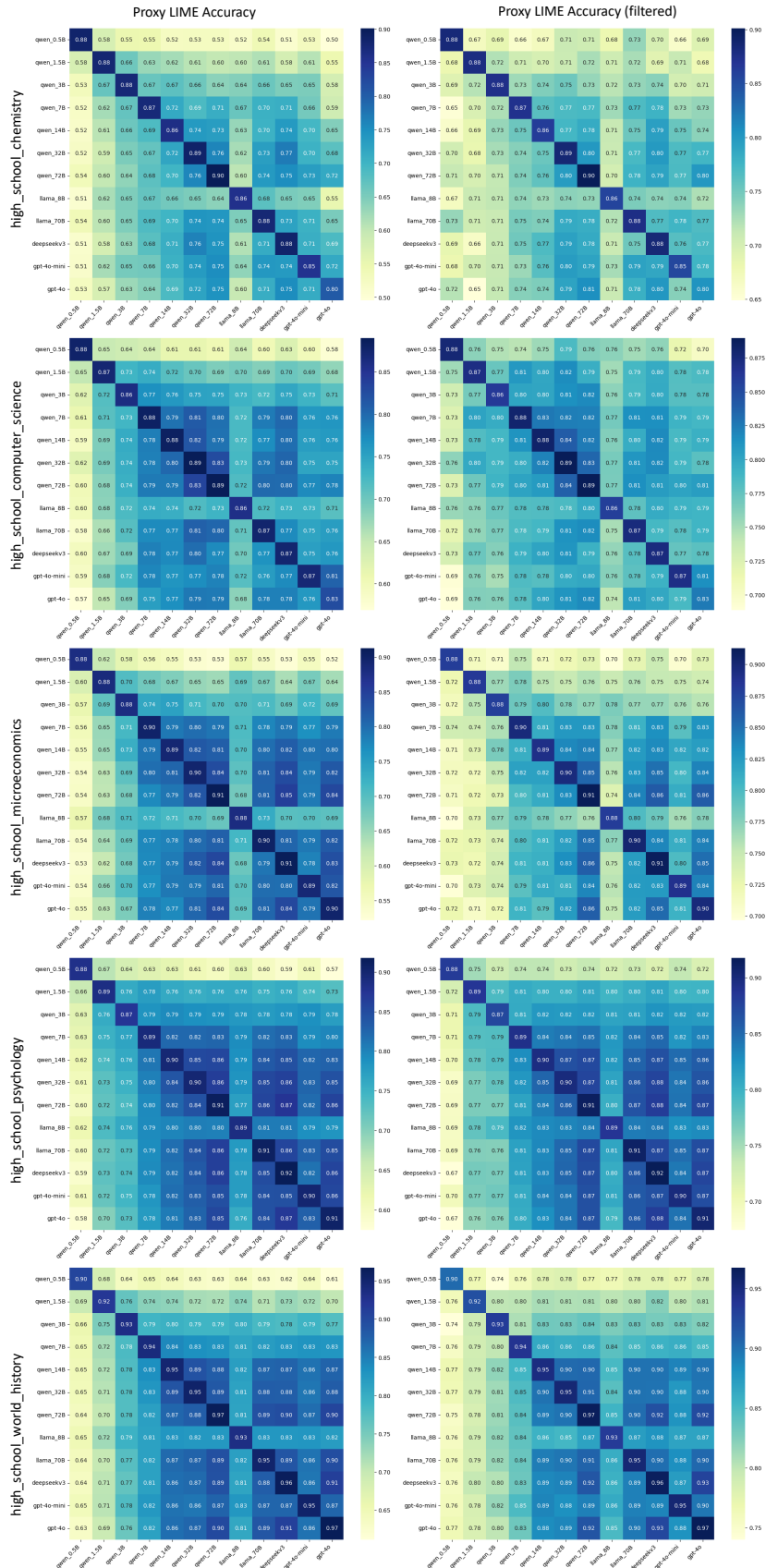


Figure 9: Accuracy of LIME proxy explanations on the multiple-choice question answering task on each subject. Each cell shows how well explanations generated by the model on the **y-axis** serve as surrogates for predicting the behavior of the model on the **x-axis**. The heatmap on the right shows results after filtering out examples where the budget-friendly and expensive models produce different predictions for the input.

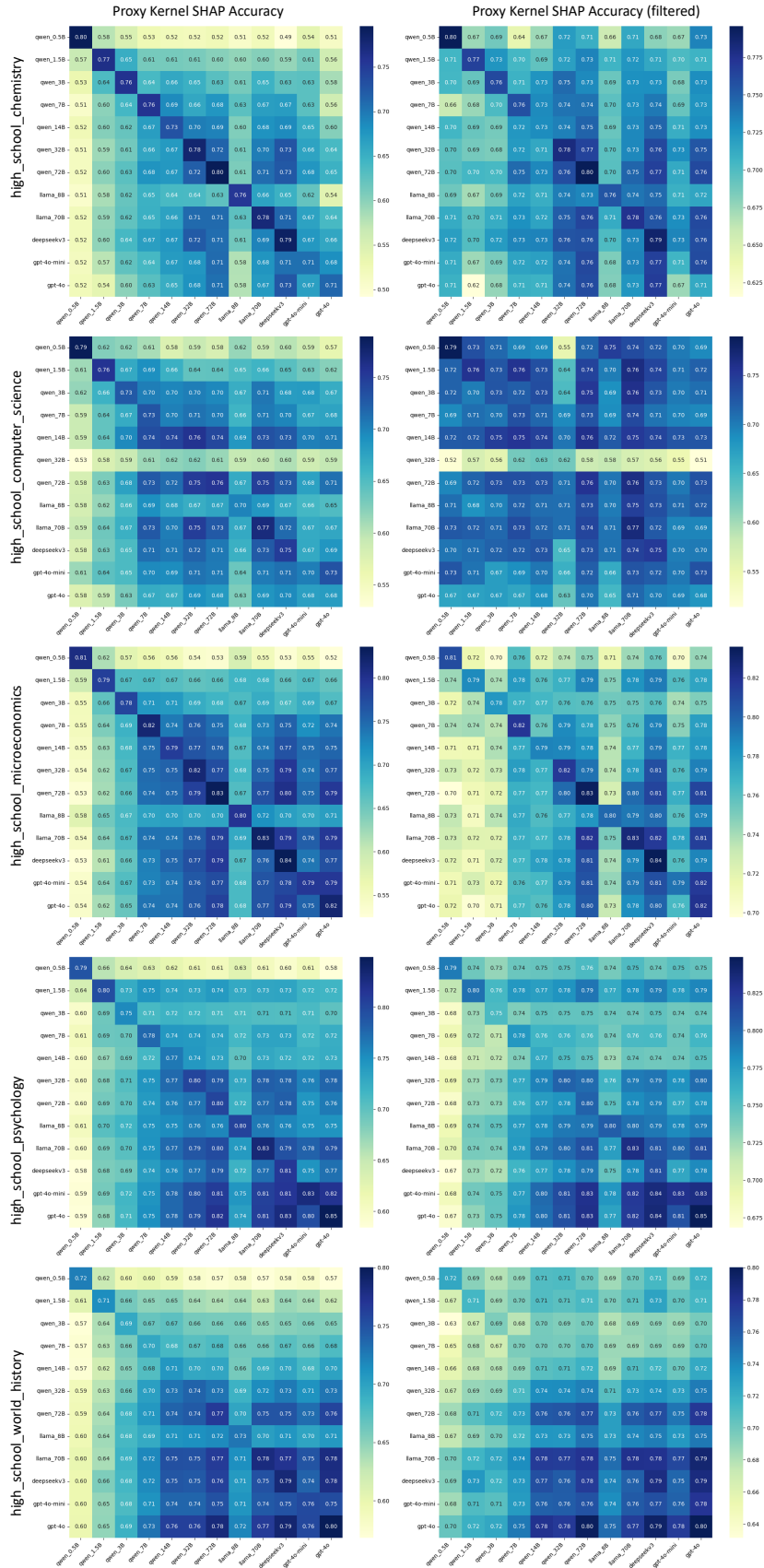


Figure 10: Accuracy of Kernel SHAP proxy explanations on the multiple-choice question answering task on each subject. Each cell shows how well explanations generated by the model on the **y-axis** serve as surrogates for predicting the behavior of the model on the **x-axis**. The heatmap on the right shows results after filtering out examples where the budget-friendly and expensive models produce different predictions for the input.

Algorithm 1: Task-level Screening for Multiple Proxy Models

Input: Target model f ; candidate proxy models $\{f'_1, \dots, f'_m\}$; dataset \mathbb{D} ; explanation technique t ; fidelity threshold τ ; confidence level $1 - \delta$; maximum sample size N .

Output: Screening decisions $\{s_{\text{task}}^{\tau, \delta}(f'_j; f, \mathbb{D})\}_{j=1}^m$.

foreach proxy model f'_j **do**

- Initialize $n \leftarrow 0$, paired difference set $\mathcal{D}_j \leftarrow \emptyset$;
- Define $\mathbb{D}'_j = \{\mathbf{x} \in \mathbb{D} : f(\mathbf{x}) = f'_j(\mathbf{x})\}$;
- while** decision not reached and $n < N$ **do**
 - Sample \mathbf{x}_i from \mathbb{D}'_j via rejection sampling;
 - Compute fidelities $q_{\text{proxy}}(\mathbf{x}_i)$ and $q_{\text{oracle}}(\mathbf{x}_i)$ with Buffer \mathcal{B} and update \mathcal{B} ;
 - Form difference $d_i = q_{\text{proxy}}(\mathbf{x}_i) - \tau q_{\text{oracle}}(\mathbf{x}_i)$;
 - Update \hat{d}_j and variance $s_{d,j}^2$;
 - Construct $(1 - \delta)$ confidence interval for μ_d ;
 - if** interval > 0 **then**
 - Accept H_1 ; set $s_{\text{task}}^{\tau, \delta}(f'_j; f, \mathbb{D}) = 1$;
 - else**
 - if** interval < 0 **then**
 - Accept H_0 ; set $s_{\text{task}}^{\tau, \delta}(f'_j; f, \mathbb{D}) = 0$;
 - else**
 - Continue sampling;
- if** no decision after N samples **then**
 - Set $s_{\text{task}}^{\tau, \delta}(f'_j; f, \mathbb{D}) = 0$;

Table 6: Accuracy of proxy LIME explanations on high school chemistry of MMLU datasets: each value shows how well LIME explanations generated by the model on the **left** serve as surrogates for predicting the behavior of the model on the **top**.

	Qwen 0.5B	Qwen 1.5B	Qwen 3B	Qwen 7B	Qwen 14B	Qwen 32B
Qwen 0.5B	88.40% \pm 1.21	57.69% \pm 3.96	54.85% \pm 4.04	54.68% \pm 4.00	52.45% \pm 3.82	52.60% \pm 4.07
Qwen 1.5B	57.69% \pm 3.72	87.85% \pm 1.19	66.16% \pm 3.41	62.99% \pm 3.57	62.17% \pm 3.46	60.66% \pm 3.84
Qwen 3B	53.33% \pm 4.11	66.66% \pm 3.28	87.50% \pm 1.18	66.64% \pm 3.30	67.46% \pm 3.23	66.13% \pm 3.72
Qwen 7B	51.98% \pm 4.20	62.08% \pm 3.75	66.84% \pm 3.50	87.32% \pm 1.20	71.58% \pm 3.05	68.92% \pm 3.59
Qwen 14B	51.61% \pm 4.03	60.55% \pm 3.65	66.29% \pm 3.39	68.77% \pm 3.27	86.26% \pm 1.28	73.70% \pm 3.08
Qwen 32B	52.17% \pm 4.19	58.59% \pm 3.99	65.03% \pm 3.61	66.96% \pm 3.42	72.10% \pm 3.02	88.61% \pm 1.20
Qwen 72B	53.53% \pm 4.19	59.96% \pm 3.79	63.63% \pm 3.65	67.55% \pm 3.39	69.91% \pm 3.09	75.94% \pm 3.11
Llama 8B	50.80% \pm 3.93	61.74% \pm 3.72	64.80% \pm 3.29	66.87% \pm 3.31	65.83% \pm 3.20	64.98% \pm 3.59
Llama 70B	53.71% \pm 4.05	60.43% \pm 3.89	64.73% \pm 3.62	68.63% \pm 3.25	69.92% \pm 3.13	74.35% \pm 3.07
DeepSeekV3	51.13% \pm 4.21	58.08% \pm 3.92	63.28% \pm 3.56	67.76% \pm 3.37	70.82% \pm 3.05	76.40% \pm 2.83
GPT-4o Mini	51.46% \pm 4.05	62.03% \pm 3.75	65.46% \pm 3.45	65.75% \pm 3.47	70.48% \pm 3.03	73.60% \pm 3.10
GPT-4o	52.82% \pm 4.21	57.45% \pm 3.77	62.72% \pm 3.68	64.12% \pm 3.53	68.97% \pm 3.08	72.44% \pm 3.33

	Qwen 72B	Llama 8B	Llama 70B	DeepSeekV3	GPT-4o Mini	GPT-4o
Qwen 0.5B	52.58% \pm 4.19	51.61% \pm 3.77	53.97% \pm 3.96	50.99% \pm 4.16	52.96% \pm 3.97	49.53% \pm 4.38
Qwen 1.5B	59.95% \pm 3.88	60.28% \pm 3.54	61.35% \pm 3.69	58.04% \pm 3.91	60.91% \pm 3.74	54.69% \pm 4.35
Qwen 3B	63.84% \pm 3.84	64.41% \pm 3.27	66.42% \pm 3.48	64.77% \pm 3.63	64.92% \pm 3.57	57.94% \pm 4.43
Qwen 7B	70.98% \pm 3.49	66.58% \pm 3.29	70.46% \pm 3.36	70.82% \pm 3.30	65.65% \pm 3.76	58.59% \pm 4.68
Qwen 14B	73.27% \pm 3.13	63.13% \pm 3.46	70.42% \pm 3.20	73.70% \pm 2.96	69.61% \pm 3.24	64.58% \pm 3.94
Qwen 32B	76.10% \pm 3.20	61.95% \pm 3.55	73.08% \pm 3.20	77.07% \pm 2.80	70.42% \pm 3.46	67.63% \pm 4.15
Qwen 72B	90.10% \pm 1.10	60.33% \pm 3.66	73.63% \pm 3.09	75.14% \pm 3.08	73.16% \pm 3.14	71.58% \pm 3.78
Llama 8B	63.84% \pm 3.67	85.70% \pm 1.20	67.60% \pm 3.33	65.18% \pm 3.48	64.61% \pm 3.58	55.19% \pm 4.38
Llama 70B	74.00% \pm 3.09	64.75% \pm 3.37	87.69% \pm 1.18	72.60% \pm 3.19	70.56% \pm 3.39	65.14% \pm 4.37
DeepSeekV3	74.51% \pm 3.27	61.24% \pm 3.64	71.39% \pm 3.24	88.42% \pm 1.25	70.83% \pm 3.33	68.90% \pm 3.99
GPT-4o Mini	75.06% \pm 3.10	63.59% \pm 3.49	73.85% \pm 2.97	73.68% \pm 3.09	85.47% \pm 1.73	71.61% \pm 3.48
GPT-4o	74.68% \pm 3.23	59.56% \pm 3.63	70.98% \pm 3.30	75.32% \pm 3.00	71.39% \pm 3.16	80.39% \pm 2.61

Table 7: Accuracy of proxy **filtered** LIME explanations on high school chemistry of MMLU datasets: each value shows how well LIME explanations generated by the model on the **left** serve as surrogates for predicting the behavior of the model on the **top**.

	Qwen 0.5B	Qwen 1.5B	Qwen 3B	Qwen 7B	Qwen 14B	Qwen 32B
Qwen 0.5B	88.40% \pm 1.21	66.96% \pm 5.07	68.54% \pm 5.25	66.02% \pm 5.54	66.96% \pm 6.10	70.93% \pm 5.80
Qwen 1.5B	68.20% \pm 4.93	87.85% \pm 1.19	72.08% \pm 3.90	70.61% \pm 4.30	69.95% \pm 4.25	70.82% \pm 4.89
Qwen 3B	69.24% \pm 5.44	71.96% \pm 4.18	87.50% \pm 1.18	72.88% \pm 3.84	74.31% \pm 3.90	75.15% \pm 4.18
Qwen 7B	65.19% \pm 5.96	69.80% \pm 4.61	72.27% \pm 3.87	87.32% \pm 1.20	76.26% \pm 3.43	76.91% \pm 3.71
Qwen 14B	66.06% \pm 6.58	68.60% \pm 4.57	73.32% \pm 3.84	75.29% \pm 3.47	86.26% \pm 1.28	77.33% \pm 3.27
Qwen 32B	70.37% \pm 6.29	68.36% \pm 5.19	72.64% \pm 4.19	74.01% \pm 3.68	75.40% \pm 3.27	88.61% \pm 1.20
Qwen 72B	71.14% \pm 5.77	69.95% \pm 4.55	71.34% \pm 4.17	74.25% \pm 3.53	75.85% \pm 3.22	79.72% \pm 3.06
Llama 8B	66.86% \pm 6.08	70.93% \pm 4.59	71.45% \pm 3.90	73.62% \pm 3.67	73.00% \pm 3.51	73.83% \pm 3.68
Llama 70B	73.26% \pm 5.44	70.58% \pm 4.71	70.97% \pm 4.28	74.65% \pm 3.81	74.30% \pm 3.56	78.56% \pm 2.97
DeepSeekV3	68.55% \pm 6.21	66.40% \pm 5.09	71.05% \pm 4.44	75.06% \pm 3.47	76.81% \pm 3.26	79.35% \pm 2.76
GPT-4o Mini	68.20% \pm 5.87	70.35% \pm 4.74	71.08% \pm 3.81	73.10% \pm 4.00	76.30% \pm 3.46	79.71% \pm 3.14
GPT-4o	71.88% \pm 5.40	64.87% \pm 4.72	71.27% \pm 4.24	73.99% \pm 3.63	74.42% \pm 3.52	79.07% \pm 3.19

	Qwen 72B	Llama 8B	Llama 70B	DeepSeekV3	GPT-4o Mini	GPT-4o
Qwen 0.5B	70.60% \pm 5.61	67.99% \pm 5.86	73.40% \pm 5.29	69.92% \pm 5.95	66.09% \pm 5.76	69.36% \pm 5.97
Qwen 1.5B	72.49% \pm 4.45	70.68% \pm 4.27	72.49% \pm 4.44	69.08% \pm 4.80	71.08% \pm 4.65	67.79% \pm 4.84
Qwen 3B	73.28% \pm 4.29	71.73% \pm 3.75	73.36% \pm 4.24	73.85% \pm 4.31	70.25% \pm 4.09	70.51% \pm 4.75
Qwen 7B	77.16% \pm 3.65	72.95% \pm 3.77	76.81% \pm 3.75	77.72% \pm 3.55	72.81% \pm 4.21	73.42% \pm 4.40
Qwen 14B	78.43% \pm 3.17	71.18% \pm 3.60	75.27% \pm 3.53	79.44% \pm 3.17	75.43% \pm 3.74	73.76% \pm 4.00
Qwen 32B	80.01% \pm 3.12	70.98% \pm 3.73	77.16% \pm 3.01	79.91% \pm 2.80	76.83% \pm 3.39	77.47% \pm 3.48
Qwen 72B	90.10% \pm 1.10	70.20% \pm 3.66	77.73% \pm 3.11	79.11% \pm 3.07	76.91% \pm 3.34	80.03% \pm 3.01
Llama 8B	73.49% \pm 3.76	85.70% \pm 1.20	74.47% \pm 3.63	73.75% \pm 3.66	73.98% \pm 3.72	72.32% \pm 3.99
Llama 70B	78.24% \pm 3.04	71.99% \pm 3.72	87.69% \pm 1.18	76.71% \pm 3.36	77.53% \pm 3.22	76.71% \pm 3.66
DeepSeekV3	78.48% \pm 3.25	70.90% \pm 3.66	75.12% \pm 3.35	88.42% \pm 1.25	76.31% \pm 3.43	77.03% \pm 3.40
GPT-4o Mini	79.15% \pm 3.22	72.64% \pm 3.70	79.25% \pm 2.92	78.83% \pm 3.34	85.47% \pm 1.73	77.58% \pm 3.36
GPT-4o	80.69% \pm 2.98	70.96% \pm 3.82	78.01% \pm 3.05	80.09% \pm 2.90	73.96% \pm 3.47	80.39% \pm 2.61

Table 8: Accuracy of proxy LIME explanations on high school computer science of MMLU datasets: each value shows how well LIME explanations generated by the model on the **left** serve as surrogates for predicting the behavior of the model on the **top**.

	Qwen 0.5B	Qwen 1.5B	Qwen 3B	Qwen 7B	Qwen 14B	Qwen 32B
Qwen 0.5B	87.75% \pm 1.77	64.64% \pm 5.28	64.23% \pm 4.75	63.54% \pm 5.23	61.44% \pm 5.29	61.47% \pm 5.26
Qwen 1.5B	65.08% \pm 5.40	87.13% \pm 1.75	73.00% \pm 4.29	73.94% \pm 4.41	71.53% \pm 4.56	70.29% \pm 4.87
Qwen 3B	62.31% \pm 5.32	71.57% \pm 4.48	86.11% \pm 1.81	76.87% \pm 3.56	76.13% \pm 3.51	75.05% \pm 4.09
Qwen 7B	61.25% \pm 5.58	71.35% \pm 4.54	72.84% \pm 4.20	88.08% \pm 1.71	79.37% \pm 3.53	81.29% \pm 3.20
Qwen 14B	59.28% \pm 5.70	68.95% \pm 4.72	74.12% \pm 3.50	78.41% \pm 3.68	88.21% \pm 1.73	81.78% \pm 3.56
Qwen 32B	62.31% \pm 5.70	69.15% \pm 5.00	73.90% \pm 3.69	78.19% \pm 3.69	80.13% \pm 3.65	88.88% \pm 1.76
Qwen 72B	60.20% \pm 5.70	68.31% \pm 4.99	73.58% \pm 3.78	78.79% \pm 3.39	78.75% \pm 3.71	83.34% \pm 2.98
Llama 8B	59.99% \pm 5.54	68.22% \pm 4.68	72.18% \pm 3.75	73.98% \pm 4.23	73.72% \pm 4.14	71.93% \pm 4.70
Llama 70B	58.14% \pm 5.65	66.28% \pm 5.00	71.51% \pm 4.37	77.35% \pm 3.70	77.30% \pm 4.02	80.73% \pm 3.51
DeepSeekV3	59.53% \pm 5.73	66.98% \pm 5.06	69.21% \pm 4.49	78.17% \pm 3.44	77.44% \pm 3.88	79.76% \pm 3.66
GPT-4o Mini	59.05% \pm 5.77	68.49% \pm 4.76	72.46% \pm 4.12	77.73% \pm 3.65	76.53% \pm 4.06	77.04% \pm 4.18
GPT-4o	56.87% \pm 5.83	65.23% \pm 5.27	68.73% \pm 4.49	75.43% \pm 3.69	77.01% \pm 3.86	78.82% \pm 3.61

	Qwen 72B	Llama 8B	Llama 70B	DeepSeekV3	GPT-4o Mini	GPT-4o
Qwen 0.5B	60.62% \pm 5.42	64.07% \pm 4.89	60.28% \pm 5.42	62.83% \pm 5.49	60.11% \pm 5.55	57.56% \pm 5.88
Qwen 1.5B	69.01% \pm 4.93	69.60% \pm 4.66	68.53% \pm 5.05	70.21% \pm 4.99	69.42% \pm 4.95	67.86% \pm 5.52
Qwen 3B	74.92% \pm 3.94	73.27% \pm 3.85	72.48% \pm 4.47	74.65% \pm 4.14	73.18% \pm 4.34	71.19% \pm 4.95
Qwen 7B	79.54% \pm 3.71	72.38% \pm 4.34	78.66% \pm 3.73	80.10% \pm 3.56	76.07% \pm 4.16	76.38% \pm 4.24
Qwen 14B	79.38% \pm 3.85	72.38% \pm 4.14	77.14% \pm 4.07	79.62% \pm 3.84	75.57% \pm 4.47	76.00% \pm 4.78
Qwen 32B	82.74% \pm 3.23	72.57% \pm 4.52	78.99% \pm 3.98	80.33% \pm 3.87	74.80% \pm 4.71	74.89% \pm 4.75
Qwen 72B	88.95% \pm 1.67	71.99% \pm 4.36	79.98% \pm 3.45	79.87% \pm 4.03	77.39% \pm 4.09	78.00% \pm 4.29
Llama 8B	73.12% \pm 4.52	85.79% \pm 1.75	72.08% \pm 4.73	73.19% \pm 4.55	73.25% \pm 4.47	71.36% \pm 5.12
Llama 70B	80.27% \pm 3.58	70.69% \pm 4.71	87.45% \pm 2.10	77.40% \pm 4.43	74.81% \pm 4.53	75.62% \pm 4.76
DeepSeekV3	77.38% \pm 4.29	69.87% \pm 4.60	76.71% \pm 4.28	87.32% \pm 2.21	75.41% \pm 4.66	76.09% \pm 4.56
GPT-4o Mini	78.12% \pm 4.03	71.51% \pm 4.57	75.75% \pm 4.20	77.36% \pm 4.45	87.03% \pm 2.25	80.57% \pm 4.04
GPT-4o	78.76% \pm 3.66	68.20% \pm 4.56	78.22% \pm 3.46	78.18% \pm 3.86	76.11% \pm 4.20	82.58% \pm 3.51

Table 9: Accuracy of proxy **filtered** LIME explanations on high school computer science of MMLU datasets: each value shows how well LIME explanations generated by the model on the **left** serve as surrogates for predicting the behavior of the model on the **top**.

	Qwen 0.5B	Qwen 1.5B	Qwen 3B	Qwen 7B	Qwen 14B	Qwen 32B
Qwen 0.5B	87.75% \pm 1.77	75.97% \pm 5.91	74.61% \pm 5.48	74.28% \pm 6.82	75.35% \pm 6.90	78.50% \pm 6.19
Qwen 1.5B	75.29% \pm 5.73	87.13% \pm 1.75	77.29% \pm 4.67	80.88% \pm 4.18	79.97% \pm 4.45	81.58% \pm 4.05
Qwen 3B	73.31% \pm 5.61	76.74% \pm 4.37	86.11% \pm 1.81	80.15% \pm 3.70	80.01% \pm 3.81	81.41% \pm 3.90
Qwen 7B	72.53% \pm 6.77	80.23% \pm 3.89	79.53% \pm 3.88	88.08% \pm 1.71	82.60% \pm 3.49	82.34% \pm 3.39
Qwen 14B	72.79% \pm 7.00	78.21% \pm 4.43	78.82% \pm 3.96	81.21% \pm 3.69	88.21% \pm 1.73	84.08% \pm 3.26
Qwen 32B	75.92% \pm 6.52	79.77% \pm 4.14	78.79% \pm 4.17	79.52% \pm 3.72	82.13% \pm 3.48	88.88% \pm 1.76
Qwen 72B	72.53% \pm 7.12	77.10% \pm 4.61	79.00% \pm 3.99	80.20% \pm 3.59	80.74% \pm 3.73	83.79% \pm 3.00
Llama 8B	75.51% \pm 6.51	75.91% \pm 4.53	77.24% \pm 3.88	78.13% \pm 4.38	78.28% \pm 4.35	78.50% \pm 4.63
Llama 70B	71.92% \pm 6.93	75.73% \pm 4.71	76.56% \pm 4.73	78.46% \pm 4.00	78.79% \pm 4.19	81.30% \pm 3.65
DeepSeekV3	72.91% \pm 6.81	77.23% \pm 4.76	76.21% \pm 4.67	79.15% \pm 3.70	80.15% \pm 3.63	81.15% \pm 3.50
GPT-4o Mini	69.10% \pm 7.67	76.07% \pm 4.74	74.98% \pm 4.58	78.29% \pm 4.04	77.98% \pm 4.68	79.63% \pm 4.57
GPT-4o	68.86% \pm 7.57	76.25% \pm 4.76	76.19% \pm 4.36	78.01% \pm 3.76	80.03% \pm 4.01	81.12% \pm 3.56

	Qwen 72B	Llama 8B	Llama 70B	DeepSeekV3	GPT-4o Mini	GPT-4o
Qwen 0.5B	76.28% \pm 6.99	75.93% \pm 5.83	75.21% \pm 7.04	75.81% \pm 6.80	71.57% \pm 7.71	70.18% \pm 8.21
Qwen 1.5B	79.39% \pm 4.55	75.18% \pm 4.75	78.71% \pm 4.74	79.69% \pm 4.79	78.06% \pm 4.97	78.48% \pm 4.95
Qwen 3B	81.80% \pm 3.83	75.92% \pm 3.95	78.62% \pm 4.57	79.74% \pm 4.43	77.98% \pm 4.41	77.99% \pm 4.81
Qwen 7B	82.25% \pm 3.60	76.83% \pm 4.44	81.41% \pm 3.74	81.49% \pm 3.80	79.14% \pm 4.20	78.80% \pm 4.43
Qwen 14B	82.50% \pm 3.53	76.25% \pm 4.29	79.61% \pm 4.06	81.77% \pm 3.77	78.62% \pm 4.79	79.35% \pm 4.72
Qwen 32B	83.49% \pm 3.25	76.69% \pm 4.56	81.05% \pm 3.72	81.65% \pm 3.77	78.80% \pm 4.93	77.88% \pm 4.60
Qwen 72B	88.95% \pm 1.67	76.58% \pm 4.39	81.47% \pm 3.34	80.65% \pm 3.98	80.23% \pm 4.12	80.59% \pm 3.97
Llama 8B	79.71% \pm 4.31	85.79% \pm 1.75	77.65% \pm 4.83	79.62% \pm 4.37	79.11% \pm 4.31	78.94% \pm 4.84
Llama 70B	81.61% \pm 3.44	74.97% \pm 4.77	87.45% \pm 2.10	78.72% \pm 4.51	78.01% \pm 4.70	78.94% \pm 4.43
DeepSeekV3	79.27% \pm 4.08	75.64% \pm 4.38	78.01% \pm 4.43	87.32% \pm 2.21	77.47% \pm 4.98	77.82% \pm 4.52
GPT-4o Mini	79.87% \pm 4.31	76.12% \pm 4.51	77.77% \pm 4.42	79.18% \pm 4.67	87.03% \pm 2.25	81.47% \pm 4.24
GPT-4o	81.72% \pm 3.38	74.17% \pm 4.64	80.52% \pm 3.56	79.88% \pm 3.92	78.63% \pm 4.44	82.58% \pm 3.51

Table 10: Accuracy of proxy LIME explanations on high school microeconomics of MMLU datasets: each value shows how well LIME explanations generated by the model on the **left** serve as surrogates for predicting the behavior of the model on the **top**.

	Qwen 0.5B	Qwen 1.5B	Qwen 3B	Qwen 7B	Qwen 14B	Qwen 32B
Qwen 0.5B	87.93% \pm 1.08	61.79% \pm 3.38	58.21% \pm 3.36	55.88% \pm 3.79	55.37% \pm 3.68	53.39% \pm 3.77
Qwen 1.5B	59.72% \pm 3.53	88.26% \pm 1.06	70.39% \pm 2.95	68.05% \pm 3.40	66.76% \pm 3.38	65.19% \pm 3.53
Qwen 3B	57.43% \pm 3.60	69.15% \pm 3.10	87.87% \pm 1.17	73.62% \pm 3.04	74.55% \pm 2.83	71.28% \pm 3.03
Qwen 7B	56.09% \pm 3.74	65.12% \pm 3.44	71.40% \pm 3.02	89.77% \pm 1.11	79.03% \pm 2.51	80.10% \pm 2.36
Qwen 14B	55.36% \pm 3.79	64.97% \pm 3.48	72.78% \pm 2.86	79.30% \pm 2.52	89.15% \pm 1.13	82.18% \pm 2.19
Qwen 32B	54.31% \pm 3.81	62.69% \pm 3.57	69.43% \pm 3.03	79.95% \pm 2.34	80.79% \pm 2.28	89.61% \pm 1.18
Qwen 72B	54.47% \pm 3.78	62.55% \pm 3.58	67.56% \pm 3.12	77.28% \pm 2.72	79.18% \pm 2.51	82.41% \pm 2.12
Llama 8B	57.24% \pm 3.51	67.74% \pm 3.05	70.65% \pm 2.93	72.40% \pm 3.22	71.27% \pm 3.16	70.09% \pm 3.26
Llama 70B	54.14% \pm 3.76	64.38% \pm 3.55	68.67% \pm 3.10	77.43% \pm 2.65	78.06% \pm 2.63	80.20% \pm 2.49
DeepSeekV3	53.42% \pm 3.90	61.95% \pm 3.67	67.78% \pm 3.29	77.37% \pm 2.77	78.74% \pm 2.63	82.08% \pm 2.21
GPT-4o Mini	53.96% \pm 3.71	65.55% \pm 3.33	70.40% \pm 2.96	76.70% \pm 2.70	78.93% \pm 2.47	79.09% \pm 2.48
GPT-4o	54.86% \pm 3.86	62.63% \pm 3.55	67.03% \pm 3.31	78.17% \pm 2.61	77.30% \pm 2.74	80.74% \pm 2.44

	Qwen 72B	Llama 8B	Llama 70B	DeepSeekV3	GPT-4o Mini	GPT-4o
Qwen 0.5B	52.72% \pm 3.98	57.12% \pm 3.60	54.63% \pm 3.81	52.68% \pm 4.03	55.24% \pm 3.67	52.17% \pm 3.98
Qwen 1.5B	64.62% \pm 3.63	69.07% \pm 3.03	67.05% \pm 3.46	63.84% \pm 3.72	67.33% \pm 3.25	64.29% \pm 3.56
Qwen 3B	70.11% \pm 3.30	70.33% \pm 3.11	70.82% \pm 3.24	68.82% \pm 3.47	71.80% \pm 3.07	69.00% \pm 3.39
Qwen 7B	79.31% \pm 2.69	70.79% \pm 3.17	77.66% \pm 2.72	79.16% \pm 2.77	76.56% \pm 2.75	78.89% \pm 2.76
Qwen 14B	81.44% \pm 2.57	70.45% \pm 3.15	79.91% \pm 2.58	81.54% \pm 2.52	79.55% \pm 2.45	79.87% \pm 2.67
Qwen 32B	83.54% \pm 2.29	69.52% \pm 3.13	81.12% \pm 2.51	83.73% \pm 2.23	78.92% \pm 2.48	82.13% \pm 2.38
Qwen 72B	91.30% \pm 1.03	67.88% \pm 3.22	80.94% \pm 2.56	85.08% \pm 2.11	78.87% \pm 2.53	84.04% \pm 2.21
Llama 8B	68.56% \pm 3.39	88.01% \pm 1.17	73.17% \pm 3.05	69.80% \pm 3.51	69.99% \pm 3.23	69.48% \pm 3.39
Llama 70B	81.23% \pm 2.64	71.47% \pm 3.04	90.14% \pm 1.18	80.90% \pm 2.68	78.95% \pm 2.61	81.89% \pm 2.47
DeepSeekV3	84.24% \pm 2.24	68.40% \pm 3.33	79.26% \pm 2.77	91.10% \pm 1.26	78.07% \pm 2.76	83.29% \pm 2.38
GPT-4o Mini	80.84% \pm 2.57	69.68% \pm 3.16	80.13% \pm 2.58	79.90% \pm 2.69	88.90% \pm 1.20	82.35% \pm 2.31
GPT-4o	83.78% \pm 2.33	69.32% \pm 3.23	80.61% \pm 2.55	84.00% \pm 2.27	79.43% \pm 2.49	89.74% \pm 1.35

Table 11: Accuracy of proxy **filtered** LIME explanations on high school microeconomics of MMLU datasets: each value shows how well LIME explanations generated by the model on the **left** serve as surrogates for predicting the behavior of the model on the **top**.

	Qwen 0.5B	Qwen 1.5B	Qwen 3B	Qwen 7B	Qwen 14B	Qwen 32B
Qwen 0.5B	87.93% \pm 1.08	71.42% \pm 3.82	70.66% \pm 3.94	75.31% \pm 3.72	71.32% \pm 4.38	72.11% \pm 4.26
Qwen 1.5B	72.28% \pm 3.80	88.26% \pm 1.06	76.60% \pm 2.96	77.90% \pm 2.79	75.49% \pm 3.09	74.98% \pm 3.17
Qwen 3B	71.68% \pm 4.06	75.48% \pm 3.01	87.87% \pm 1.17	78.61% \pm 2.86	79.81% \pm 2.63	77.66% \pm 2.90
Qwen 7B	74.44% \pm 3.93	74.49% \pm 3.07	75.93% \pm 3.03	89.77% \pm 1.11	81.19% \pm 2.52	82.64% \pm 2.21
Qwen 14B	71.16% \pm 4.62	73.29% \pm 3.36	77.97% \pm 2.79	81.01% \pm 2.56	89.15% \pm 1.13	83.69% \pm 2.22
Qwen 32B	71.51% \pm 4.42	71.62% \pm 3.45	74.99% \pm 3.08	82.05% \pm 2.26	82.01% \pm 2.35	89.61% \pm 1.18
Qwen 72B	71.15% \pm 4.35	72.15% \pm 3.44	73.10% \pm 3.10	80.02% \pm 2.51	81.25% \pm 2.32	83.41% \pm 2.07
Llama 8B	69.67% \pm 4.22	73.13% \pm 2.98	77.13% \pm 2.97	79.04% \pm 2.70	78.07% \pm 2.77	77.14% \pm 2.89
Llama 70B	72.36% \pm 4.08	72.67% \pm 3.45	73.77% \pm 3.20	79.87% \pm 2.48	80.70% \pm 2.45	82.09% \pm 2.30
DeepSeekV3	72.62% \pm 4.39	72.14% \pm 3.47	74.21% \pm 3.28	80.56% \pm 2.55	80.91% \pm 2.47	83.19% \pm 2.18
GPT-4o Mini	69.86% \pm 4.43	73.41% \pm 3.36	74.36% \pm 3.09	79.30% \pm 2.54	81.40% \pm 2.31	81.06% \pm 2.39
GPT-4o	72.41% \pm 4.31	70.87% \pm 3.55	72.07% \pm 3.43	80.59% \pm 2.52	79.33% \pm 2.65	82.50% \pm 2.26

	Qwen 72B	Llama 8B	Llama 70B	DeepSeekV3	GPT-4o Mini	GPT-4o
Qwen 0.5B	73.13% \pm 4.20	69.84% \pm 4.17	72.93% \pm 4.15	74.78% \pm 4.25	70.34% \pm 4.34	73.23% \pm 4.25
Qwen 1.5B	75.76% \pm 3.21	74.88% \pm 2.90	75.81% \pm 3.27	75.16% \pm 3.25	75.07% \pm 3.18	74.41% \pm 3.21
Qwen 3B	77.03% \pm 3.02	77.87% \pm 2.94	76.86% \pm 3.11	76.90% \pm 3.21	76.24% \pm 3.02	75.66% \pm 3.23
Qwen 7B	82.62% \pm 2.34	77.60% \pm 2.78	80.77% \pm 2.51	83.14% \pm 2.33	79.40% \pm 2.57	82.99% \pm 2.30
Qwen 14B	84.06% \pm 2.23	76.78% \pm 2.95	82.49% \pm 2.42	83.49% \pm 2.39	81.62% \pm 2.36	82.31% \pm 2.44
Qwen 32B	85.46% \pm 1.98	75.55% \pm 3.00	82.86% \pm 2.38	84.95% \pm 2.10	80.35% \pm 2.46	83.93% \pm 2.13
Qwen 72B	91.30% \pm 1.03	73.53% \pm 3.15	83.95% \pm 2.15	86.10% \pm 2.01	81.21% \pm 2.25	85.98% \pm 1.78
Llama 8B	76.11% \pm 3.05	88.01% \pm 1.17	79.83% \pm 2.70	78.65% \pm 2.99	76.35% \pm 3.08	77.54% \pm 2.95
Llama 70B	84.99% \pm 2.05	77.32% \pm 2.79	90.14% \pm 1.18	83.70% \pm 2.30	81.08% \pm 2.46	84.05% \pm 2.21
DeepSeekV3	85.85% \pm 1.99	75.30% \pm 3.15	82.38% \pm 2.42	91.10% \pm 1.26	79.90% \pm 2.60	84.97% \pm 2.03
GPT-4o Mini	83.76% \pm 2.17	75.54% \pm 3.05	82.48% \pm 2.38	82.57% \pm 2.39	88.90% \pm 1.20	84.02% \pm 2.17
GPT-4o	85.85% \pm 1.96	75.12% \pm 3.16	82.38% \pm 2.44	85.23% \pm 2.06	80.76% \pm 2.45	89.74% \pm 1.35

Table 12: Accuracy of proxy LIME explanations on high school psychology of MMLU datasets: each value shows how well LIME explanations generated by the model on the **left** serve as surrogates for predicting the behavior of the model on the **top**.

	Qwen 0.5B	Qwen 1.5B	Qwen 3B	Qwen 7B	Qwen 14B	Qwen 32B
Qwen 0.5B	88.25% \pm 0.64	66.76% \pm 2.11	64.46% \pm 2.06	63.40% \pm 2.23	62.75% \pm 2.29	61.03% \pm 2.33
Qwen 1.5B	65.69% \pm 2.10	88.57% \pm 0.68	75.99% \pm 1.57	77.51% \pm 1.59	76.13% \pm 1.75	75.68% \pm 1.80
Qwen 3B	63.16% \pm 2.12	75.93% \pm 1.66	87.24% \pm 0.71	78.53% \pm 1.60	79.39% \pm 1.56	78.77% \pm 1.61
Qwen 7B	62.57% \pm 2.21	75.22% \pm 1.72	76.68% \pm 1.60	89.29% \pm 0.67	82.26% \pm 1.40	82.27% \pm 1.50
Qwen 14B	61.51% \pm 2.25	73.82% \pm 1.83	76.13% \pm 1.63	81.10% \pm 1.44	89.63% \pm 0.68	85.26% \pm 1.18
Qwen 32B	60.70% \pm 2.26	72.87% \pm 1.82	75.14% \pm 1.61	80.36% \pm 1.48	84.08% \pm 1.21	89.88% \pm 0.68
Qwen 72B	60.12% \pm 2.34	72.42% \pm 1.95	73.94% \pm 1.72	79.51% \pm 1.57	82.40% \pm 1.39	84.50% \pm 1.25
Llama 8B	61.59% \pm 2.21	73.76% \pm 1.83	76.16% \pm 1.60	79.36% \pm 1.58	79.93% \pm 1.57	80.45% \pm 1.51
Llama 70B	60.03% \pm 2.33	71.82% \pm 1.98	73.37% \pm 1.75	79.26% \pm 1.59	81.78% \pm 1.45	84.20% \pm 1.27
DeepSeekV3	58.92% \pm 2.33	72.55% \pm 1.99	73.64% \pm 1.76	79.44% \pm 1.61	81.52% \pm 1.50	83.68% \pm 1.36
GPT-4o Mini	60.51% \pm 2.26	72.04% \pm 1.98	74.61% \pm 1.69	78.25% \pm 1.63	81.76% \pm 1.43	83.07% \pm 1.33
GPT-4o	58.06% \pm 2.37	69.99% \pm 2.12	73.06% \pm 1.79	77.77% \pm 1.71	80.69% \pm 1.52	82.78% \pm 1.42

	Qwen 72B	Llama 8B	Llama 70B	DeepSeekV3	GPT-4o Mini	GPT-4o
Qwen 0.5B	60.22% \pm 2.51	62.79% \pm 2.21	59.91% \pm 2.50	58.71% \pm 2.55	60.59% \pm 2.42	57.47% \pm 2.59
Qwen 1.5B	76.11% \pm 1.90	76.19% \pm 1.69	75.19% \pm 1.95	75.78% \pm 1.99	74.21% \pm 1.96	73.23% \pm 2.15
Qwen 3B	78.69% \pm 1.75	78.03% \pm 1.59	77.75% \pm 1.83	78.33% \pm 1.81	78.80% \pm 1.68	77.51% \pm 1.87
Qwen 7B	82.57% \pm 1.53	79.27% \pm 1.59	81.86% \pm 1.60	82.56% \pm 1.65	79.25% \pm 1.76	79.75% \pm 1.85
Qwen 14B	85.50% \pm 1.30	78.79% \pm 1.60	83.63% \pm 1.45	84.63% \pm 1.48	82.42% \pm 1.53	82.89% \pm 1.64
Qwen 32B	86.49% \pm 1.12	78.62% \pm 1.55	85.38% \pm 1.25	86.03% \pm 1.32	82.60% \pm 1.43	84.51% \pm 1.45
Qwen 72B	91.35% \pm 0.61	77.26% \pm 1.72	85.66% \pm 1.30	87.48% \pm 1.13	82.10% \pm 1.58	85.98% \pm 1.40
Llama 8B	80.32% \pm 1.70	88.70% \pm 0.68	80.68% \pm 1.68	80.73% \pm 1.70	79.02% \pm 1.76	78.50% \pm 1.93
Llama 70B	86.29% \pm 1.26	77.96% \pm 1.68	91.05% \pm 0.65	85.62% \pm 1.41	82.91% \pm 1.53	85.07% \pm 1.49
DeepSeekV3	86.36% \pm 1.15	77.69% \pm 1.70	84.94% \pm 1.35	91.77% \pm 0.68	81.58% \pm 1.67	85.76% \pm 1.44
GPT-4o Mini	84.76% \pm 1.40	77.64% \pm 1.68	84.43% \pm 1.40	84.59% \pm 1.51	89.93% \pm 0.78	85.50% \pm 1.43
GPT-4o	85.49% \pm 1.31	75.91% \pm 1.83	84.49% \pm 1.45	87.05% \pm 1.21	83.04% \pm 1.48	90.62% \pm 0.81

Table 13: Accuracy of proxy **filtered** LIME explanations on high school psychology of MMLU datasets: each value shows how well LIME explanations generated by the model on the **left** serve as surrogates for predicting the behavior of the model on the **top**.

	Qwen 0.5B	Qwen 1.5B	Qwen 3B	Qwen 7B	Qwen 14B	Qwen 32B
Qwen 0.5B	88.25% \pm 0.64	75.04% \pm 2.10	73.04% \pm 2.18	73.87% \pm 2.18	73.82% \pm 2.35	72.81% \pm 2.41
Qwen 1.5B	72.43% \pm 2.23	88.57% \pm 0.68	79.09% \pm 1.48	80.55% \pm 1.52	80.12% \pm 1.67	80.10% \pm 1.70
Qwen 3B	70.61% \pm 2.28	79.03% \pm 1.55	87.24% \pm 0.71	80.59% \pm 1.54	82.01% \pm 1.47	81.97% \pm 1.51
Qwen 7B	70.64% \pm 2.30	78.60% \pm 1.64	78.69% \pm 1.56	89.29% \pm 0.67	83.83% \pm 1.28	84.24% \pm 1.37
Qwen 14B	70.09% \pm 2.46	77.96% \pm 1.74	78.79% \pm 1.58	82.83% \pm 1.34	89.63% \pm 0.68	86.68% \pm 1.09
Qwen 32B	68.77% \pm 2.50	76.73% \pm 1.79	77.90% \pm 1.59	82.17% \pm 1.41	85.24% \pm 1.16	89.88% \pm 0.68
Qwen 72B	69.04% \pm 2.52	76.67% \pm 1.87	76.67% \pm 1.71	81.19% \pm 1.51	83.87% \pm 1.34	85.51% \pm 1.16
Llama 8B	69.15% \pm 2.43	77.93% \pm 1.73	79.20% \pm 1.55	82.30% \pm 1.41	83.04% \pm 1.41	83.39% \pm 1.40
Llama 70B	69.17% \pm 2.59	76.41% \pm 1.87	76.37% \pm 1.72	81.32% \pm 1.51	83.14% \pm 1.40	85.05% \pm 1.24
DeepSeekV3	67.48% \pm 2.54	76.95% \pm 1.89	76.78% \pm 1.74	81.31% \pm 1.51	83.27% \pm 1.38	85.16% \pm 1.21
GPT-4o Mini	69.71% \pm 2.45	76.70% \pm 1.87	77.26% \pm 1.65	80.63% \pm 1.50	83.59% \pm 1.32	84.32% \pm 1.26
GPT-4o	67.44% \pm 2.63	75.65% \pm 1.96	76.24% \pm 1.78	80.41% \pm 1.60	82.65% \pm 1.45	84.33% \pm 1.31

	Qwen 72B	Llama 8B	Llama 70B	DeepSeekV3	GPT-4o Mini	GPT-4o
Qwen 0.5B	73.54% \pm 2.44	72.37% \pm 2.35	73.02% \pm 2.53	71.91% \pm 2.51	73.67% \pm 2.36	72.08% \pm 2.58
Qwen 1.5B	80.93% \pm 1.73	79.69% \pm 1.66	80.31% \pm 1.75	81.04% \pm 1.79	79.70% \pm 1.76	79.79% \pm 1.87
Qwen 3B	82.04% \pm 1.61	81.16% \pm 1.51	81.33% \pm 1.68	82.42% \pm 1.65	81.85% \pm 1.56	81.78% \pm 1.71
Qwen 7B	84.59% \pm 1.37	82.06% \pm 1.46	84.30% \pm 1.44	85.05% \pm 1.45	82.25% \pm 1.50	83.44% \pm 1.56
Qwen 14B	87.18% \pm 1.17	81.97% \pm 1.46	85.33% \pm 1.35	86.72% \pm 1.28	84.89% \pm 1.29	85.86% \pm 1.38
Qwen 32B	87.42% \pm 1.04	81.18% \pm 1.51	86.17% \pm 1.23	87.56% \pm 1.12	84.28% \pm 1.29	86.38% \pm 1.25
Qwen 72B	91.35% \pm 0.61	80.19% \pm 1.68	86.53% \pm 1.23	88.09% \pm 1.10	84.42% \pm 1.30	87.40% \pm 1.19
Llama 8B	83.76% \pm 1.52	88.70% \pm 0.68	83.95% \pm 1.49	84.12% \pm 1.50	82.57% \pm 1.54	82.98% \pm 1.63
Llama 70B	87.20% \pm 1.18	80.96% \pm 1.61	91.05% \pm 0.65	87.22% \pm 1.25	84.82% \pm 1.30	86.94% \pm 1.24
DeepSeekV3	86.97% \pm 1.10	80.37% \pm 1.64	86.26% \pm 1.25	91.77% \pm 0.68	84.10% \pm 1.39	87.40% \pm 1.20
GPT-4o Mini	86.67% \pm 1.17	80.70% \pm 1.59	86.04% \pm 1.22	86.66% \pm 1.30	89.93% \pm 0.78	86.88% \pm 1.29
GPT-4o	86.68% \pm 1.14	79.34% \pm 1.73	86.06% \pm 1.25	87.99% \pm 1.12	84.46% \pm 1.36	90.62% \pm 0.81

Table 14: Accuracy of proxy LIME explanations on high school world history of MMLU datasets: each value shows how well LIME explanations generated by the model on the **left** serve as surrogates for predicting the behavior of the model on the **top**.

	Qwen 0.5B	Qwen 1.5B	Qwen 3B	Qwen 7B	Qwen 14B	Qwen 32B
Qwen 0.5B	90.36% ± 0.91	68.25% ± 3.34	63.86% ± 3.73	65.07% ± 3.85	64.21% ± 3.95	63.09% ± 4.10
Qwen 1.5B	69.49% ± 3.18	91.99% ± 0.83	76.31% ± 2.98	73.84% ± 3.29	73.58% ± 3.46	72.11% ± 3.70
Qwen 3B	65.82% ± 3.52	74.68% ± 3.05	93.28% ± 0.78	79.03% ± 2.87	79.62% ± 2.87	79.05% ± 3.08
Qwen 7B	65.24% ± 3.67	72.01% ± 3.37	78.18% ± 2.93	94.01% ± 0.77	84.16% ± 2.38	83.29% ± 2.60
Qwen 14B	64.82% ± 3.70	71.56% ± 3.44	77.93% ± 2.98	83.48% ± 2.36	94.83% ± 0.74	89.08% ± 1.84
Qwen 32B	64.62% ± 3.75	71.06% ± 3.56	77.67% ± 3.03	82.73% ± 2.52	88.93% ± 1.80	95.39% ± 0.75
Qwen 72B	64.12% ± 3.82	70.28% ± 3.66	77.60% ± 3.18	81.59% ± 2.80	87.11% ± 2.16	87.85% ± 2.24
Llama 8B	65.05% ± 3.64	72.43% ± 3.34	79.46% ± 2.81	81.47% ± 2.60	82.76% ± 2.62	82.49% ± 2.75
Llama 70B	64.27% ± 3.83	70.04% ± 3.65	77.32% ± 3.10	81.53% ± 2.71	86.75% ± 2.16	87.39% ± 2.27
DeepSeekV3	63.64% ± 4.01	70.65% ± 3.73	76.50% ± 3.36	81.45% ± 2.83	86.32% ± 2.35	86.76% ± 2.45
GPT-4o Mini	64.55% ± 3.79	70.86% ± 3.61	77.83% ± 3.06	82.42% ± 2.65	86.04% ± 2.29	85.71% ± 2.56
GPT-4o	63.23% ± 3.98	69.48% ± 3.79	75.88% ± 3.42	81.55% ± 2.80	86.39% ± 2.30	87.06% ± 2.40

	Qwen 72B	Llama 8B	Llama 70B	DeepSeekV3	GPT-4o Mini	GPT-4o
Qwen 0.5B	62.71% ± 4.21	63.99% ± 3.88	62.61% ± 4.18	62.32% ± 4.38	63.97% ± 4.04	61.13% ± 4.41
Qwen 1.5B	71.75% ± 3.84	73.66% ± 3.35	71.11% ± 3.73	72.88% ± 3.83	72.11% ± 3.70	70.35% ± 3.99
Qwen 3B	79.03% ± 3.28	79.90% ± 2.84	78.50% ± 3.23	78.03% ± 3.49	79.14% ± 3.09	77.49% ± 3.56
Qwen 7B	83.03% ± 2.84	81.11% ± 2.71	82.05% ± 2.85	82.64% ± 2.96	83.01% ± 2.78	82.70% ± 2.93
Qwen 14B	87.92% ± 2.20	81.78% ± 2.72	87.24% ± 2.22	87.44% ± 2.38	86.08% ± 2.29	87.39% ± 2.36
Qwen 32B	88.52% ± 2.23	81.44% ± 2.79	87.95% ± 2.19	87.76% ± 2.42	85.73% ± 2.45	88.09% ± 2.37
Qwen 72B	96.52% ± 0.59	81.28% ± 3.01	89.10% ± 2.09	89.58% ± 2.24	86.52% ± 2.49	90.36% ± 2.15
Llama 8B	82.54% ± 3.03	93.42% ± 0.84	82.66% ± 2.82	82.56% ± 3.08	82.79% ± 2.76	82.05% ± 3.15
Llama 70B	89.32% ± 2.13	81.60% ± 2.82	95.32% ± 0.77	88.75% ± 2.26	85.94% ± 2.48	89.57% ± 2.19
DeepSeekV3	89.23% ± 2.24	81.05% ± 3.03	87.85% ± 2.36	96.40% ± 0.70	85.64% ± 2.57	91.06% ± 1.98
GPT-4o Mini	87.32% ± 2.54	82.60% ± 2.71	87.26% ± 2.32	87.26% ± 2.43	95.49% ± 0.70	87.23% ± 2.54
GPT-4o	90.03% ± 2.10	80.74% ± 3.09	88.63% ± 2.27	90.94% ± 1.97	86.06% ± 2.53	96.75% ± 0.61

Table 15: Accuracy of proxy **filtered** LIME explanations on high school world history of MMLU datasets: each value shows how well LIME explanations generated by the model on the **left** serve as surrogates for predicting the behavior of the model on the **top**.

	Qwen 0.5B	Qwen 1.5B	Qwen 3B	Qwen 7B	Qwen 14B	Qwen 32B
Qwen 0.5B	90.36% \pm 0.91	76.59% \pm 3.51	74.15% \pm 3.92	76.08% \pm 3.77	77.79% \pm 3.81	78.14% \pm 3.76
Qwen 1.5B	76.23% \pm 3.48	91.99% \pm 0.83	79.96% \pm 2.99	80.04% \pm 3.27	80.87% \pm 3.28	80.63% \pm 3.34
Qwen 3B	73.98% \pm 3.87	79.24% \pm 2.99	93.28% \pm 0.78	80.66% \pm 3.03	83.21% \pm 2.86	83.12% \pm 2.91
Qwen 7B	75.56% \pm 3.68	78.94% \pm 3.24	79.94% \pm 3.03	94.01% \pm 0.77	86.40% \pm 2.26	86.03% \pm 2.39
Qwen 14B	76.69% \pm 3.72	79.12% \pm 3.26	81.81% \pm 2.87	85.34% \pm 2.31	94.83% \pm 0.74	90.40% \pm 1.76
Qwen 32B	76.53% \pm 3.59	78.90% \pm 3.25	81.25% \pm 2.93	84.70% \pm 2.42	89.95% \pm 1.77	95.39% \pm 0.75
Qwen 72B	75.24% \pm 3.82	78.44% \pm 3.40	81.38% \pm 3.06	84.27% \pm 2.67	89.40% \pm 1.92	89.90% \pm 2.06
Llama 8B	75.64% \pm 3.70	78.88% \pm 3.29	81.76% \pm 2.81	83.92% \pm 2.59	85.68% \pm 2.55	85.21% \pm 2.64
Llama 70B	76.14% \pm 3.90	78.74% \pm 3.36	81.53% \pm 2.96	83.56% \pm 2.68	89.29% \pm 1.96	89.69% \pm 2.03
DeepSeekV3	75.74% \pm 3.92	79.76% \pm 3.37	80.39% \pm 3.29	83.34% \pm 2.82	88.67% \pm 2.08	88.98% \pm 2.11
GPT-4o Mini	76.04% \pm 3.63	78.45% \pm 3.49	81.58% \pm 2.91	84.88% \pm 2.53	88.84% \pm 2.03	88.13% \pm 2.35
GPT-4o	76.52% \pm 3.87	78.35% \pm 3.43	79.97% \pm 3.30	83.27% \pm 2.86	88.40% \pm 2.20	88.81% \pm 2.23

	Qwen 72B	Llama 8B	Llama 70B	DeepSeekV3	GPT-4o Mini	GPT-4o
Qwen 0.5B	76.94% \pm 3.95	76.53% \pm 3.79	77.58% \pm 3.98	77.58% \pm 4.04	77.23% \pm 3.77	78.31% \pm 4.00
Qwen 1.5B	80.67% \pm 3.47	80.07% \pm 3.28	80.49% \pm 3.42	82.30% \pm 3.44	80.00% \pm 3.54	80.51% \pm 3.56
Qwen 3B	83.64% \pm 3.08	82.65% \pm 2.75	83.40% \pm 2.95	82.79% \pm 3.28	83.13% \pm 2.93	82.49% \pm 3.32
Qwen 7B	86.09% \pm 2.63	84.18% \pm 2.63	85.05% \pm 2.67	85.67% \pm 2.70	85.94% \pm 2.54	85.18% \pm 2.81
Qwen 14B	90.45% \pm 1.86	85.09% \pm 2.56	89.95% \pm 1.98	89.98% \pm 2.04	88.94% \pm 2.05	89.87% \pm 2.12
Qwen 32B	90.58% \pm 2.03	84.23% \pm 2.65	89.91% \pm 2.03	89.82% \pm 2.08	87.65% \pm 2.35	89.77% \pm 2.18
Qwen 72B	96.52% \pm 0.59	85.49% \pm 2.69	90.20% \pm 2.06	91.99% \pm 1.81	88.03% \pm 2.38	92.37% \pm 1.80
Llama 8B	86.96% \pm 2.67	93.42% \pm 0.84	87.26% \pm 2.47	88.00% \pm 2.59	86.85% \pm 2.48	86.80% \pm 2.69
Llama 70B	90.72% \pm 2.03	85.99% \pm 2.50	95.32% \pm 0.77	90.08% \pm 2.12	88.27% \pm 2.24	90.49% \pm 2.13
DeepSeekV3	91.51% \pm 1.89	85.79% \pm 2.72	89.16% \pm 2.23	96.40% \pm 0.70	87.36% \pm 2.46	92.85% \pm 1.61
GPT-4o Mini	89.12% \pm 2.34	86.28% \pm 2.45	89.12% \pm 2.21	88.85% \pm 2.35	95.49% \pm 0.70	89.63% \pm 2.33
GPT-4o	91.73% \pm 1.90	84.95% \pm 2.73	89.56% \pm 2.22	92.57% \pm 1.65	88.03% \pm 2.43	96.75% \pm 0.61

Table 16: Accuracy of proxy Kernel SHAP explanations on high school chemistry of MMLU datasets: each value shows how well Kernel SHAP explanations generated by the model on the **left** serve as surrogates for predicting the behavior of the model on the **top**.

	Qwen 0.5B	Qwen 1.5B	Qwen 3B	Qwen 7B	Qwen 14B	Qwen 32B
Qwen 0.5B	79.57% ± 2.29	57.58% ± 3.83	55.11% ± 4.00	52.69% ± 3.94	52.11% ± 3.89	51.86% ± 4.08
Qwen 1.5B	56.67% ± 3.75	76.57% ± 2.48	65.22% ± 3.40	61.13% ± 3.58	61.17% ± 3.44	60.88% ± 3.62
Qwen 3B	53.17% ± 4.02	63.62% ± 3.28	76.13% ± 2.43	64.01% ± 3.36	65.89% ± 3.19	65.00% ± 3.51
Qwen 7B	50.78% ± 4.08	59.90% ± 3.71	64.21% ± 3.38	75.91% ± 2.62	68.60% ± 2.87	65.86% ± 3.49
Qwen 14B	52.47% ± 3.86	60.29% ± 3.51	62.05% ± 3.49	66.96% ± 3.20	72.97% ± 2.73	69.70% ± 3.09
Qwen 32B	51.49% ± 4.08	59.04% ± 3.87	61.37% ± 3.68	66.05% ± 3.30	67.24% ± 3.25	78.10% ± 2.47
Qwen 72B	51.61% ± 4.14	59.96% ± 3.83	62.77% ± 3.57	67.94% ± 3.28	67.42% ± 3.23	71.90% ± 3.21
Llama 8B	50.51% ± 3.97	58.38% ± 3.80	62.09% ± 3.44	64.93% ± 3.28	63.94% ± 3.23	63.82% ± 3.58
Llama 70B	52.08% ± 3.96	59.40% ± 3.81	62.38% ± 3.68	65.09% ± 3.41	66.48% ± 3.31	71.06% ± 2.96
DeepSeekV3	52.15% ± 4.19	59.74% ± 3.90	64.14% ± 3.43	66.82% ± 3.33	67.48% ± 3.20	72.30% ± 3.19
GPT-4o Mini	51.72% ± 4.16	57.42% ± 3.92	62.46% ± 3.57	64.06% ± 3.52	67.18% ± 3.27	67.59% ± 3.40
GPT-4o	52.27% ± 4.18	53.93% ± 3.98	59.94% ± 3.79	62.91% ± 3.62	65.29% ± 3.46	68.00% ± 3.54

	Qwen 72B	Llama 8B	Llama 70B	DeepSeekV3	GPT-4o Mini	GPT-4o
Qwen 0.5B	52.37% ± 4.14	50.76% ± 3.66	52.13% ± 3.91	49.19% ± 4.10	53.86% ± 3.98	51.17% ± 4.32
Qwen 1.5B	60.18% ± 3.82	59.53% ± 3.49	60.26% ± 3.66	59.45% ± 3.63	61.10% ± 3.63	55.91% ± 4.23
Qwen 3B	62.91% ± 3.69	61.13% ± 3.42	64.79% ± 3.36	62.55% ± 3.59	62.76% ± 3.48	58.50% ± 4.30
Qwen 7B	67.59% ± 3.45	62.75% ± 3.30	66.82% ± 3.26	67.06% ± 3.32	62.73% ± 3.58	55.86% ± 4.45
Qwen 14B	69.30% ± 3.31	60.49% ± 3.47	67.95% ± 3.17	68.56% ± 3.20	65.43% ± 3.31	60.26% ± 4.17
Qwen 32B	71.60% ± 3.26	61.20% ± 3.37	69.65% ± 3.18	72.82% ± 2.94	66.38% ± 3.51	63.95% ± 4.15
Qwen 72B	79.57% ± 2.54	60.77% ± 3.58	70.85% ± 3.22	72.52% ± 3.09	67.61% ± 3.48	64.93% ± 4.24
Llama 8B	62.59% ± 3.74	75.51% ± 2.39	66.46% ± 3.34	64.92% ± 3.53	62.24% ± 3.64	54.18% ± 4.47
Llama 70B	71.09% ± 3.28	62.62% ± 3.44	77.52% ± 2.58	71.37% ± 3.03	66.51% ± 3.57	63.95% ± 4.28
DeepSeekV3	70.80% ± 3.51	61.44% ± 3.55	69.22% ± 3.35	78.82% ± 2.52	67.41% ± 3.42	65.96% ± 4.14
GPT-4o Mini	70.99% ± 3.38	57.86% ± 3.68	67.77% ± 3.43	70.57% ± 3.27	70.62% ± 3.26	68.27% ± 3.72
GPT-4o	70.64% ± 3.51	57.77% ± 3.61	67.25% ± 3.43	72.61% ± 3.18	66.68% ± 3.46	71.38% ± 3.50

Table 17: Accuracy of **filtered** proxy Kernel SHAP explanations on high school chemistry of MMLU datasets: each value shows how well Kernel SHAP explanations generated by the model on the **left** serve as surrogates for predicting the behavior of the model on the **top**.

	Qwen 0.5B	Qwen 1.5B	Qwen 3B	Qwen 7B	Qwen 14B	Qwen 32B
Qwen 0.5B	79.57% \pm 2.29	67.42% \pm 4.66	68.75% \pm 5.00	64.16% \pm 5.44	67.35% \pm 6.09	72.14% \pm 5.57
Qwen 1.5B	70.51% \pm 4.43	76.57% \pm 2.48	72.57% \pm 3.55	70.46% \pm 4.17	69.40% \pm 4.06	71.97% \pm 4.24
Qwen 3B	70.46% \pm 5.07	69.16% \pm 4.09	76.13% \pm 2.43	70.79% \pm 3.82	72.63% \pm 3.75	74.54% \pm 3.63
Qwen 7B	65.90% \pm 5.45	67.53% \pm 4.51	70.18% \pm 3.63	75.91% \pm 2.62	73.07% \pm 3.32	74.09% \pm 3.54
Qwen 14B	70.50% \pm 5.14	69.12% \pm 3.96	68.63% \pm 4.02	72.42% \pm 3.56	72.97% \pm 2.73	73.58% \pm 3.15
Qwen 32B	69.56% \pm 5.99	68.68% \pm 4.63	68.40% \pm 4.41	72.28% \pm 3.74	71.45% \pm 3.55	78.10% \pm 2.47
Qwen 72B	69.70% \pm 5.71	70.44% \pm 4.73	70.33% \pm 4.11	74.52% \pm 3.21	73.21% \pm 3.53	75.92% \pm 3.11
Llama 8B	68.94% \pm 5.82	67.18% \pm 4.75	68.81% \pm 4.26	71.85% \pm 3.63	71.10% \pm 3.61	73.71% \pm 3.50
Llama 70B	71.21% \pm 5.34	69.64% \pm 4.36	71.16% \pm 4.09	72.81% \pm 3.65	71.75% \pm 3.61	75.07% \pm 2.93
DeepSeekV3	71.98% \pm 5.65	69.87% \pm 4.53	72.20% \pm 3.88	73.35% \pm 3.59	73.42% \pm 3.57	75.62% \pm 3.13
GPT-4o Mini	71.25% \pm 5.45	67.38% \pm 4.84	68.52% \pm 3.98	71.75% \pm 4.04	71.94% \pm 3.97	74.18% \pm 3.69
GPT-4o	70.86% \pm 5.54	61.56% \pm 5.10	67.62% \pm 4.67	70.94% \pm 4.29	70.84% \pm 4.16	74.26% \pm 3.76

	Qwen 72B	Llama 8B	Llama 70B	DeepSeekV3	GPT-4o Mini	GPT-4o
Qwen 0.5B	71.04% \pm 5.32	65.76% \pm 5.67	71.43% \pm 5.32	67.91% \pm 6.00	67.45% \pm 5.58	73.38% \pm 5.06
Qwen 1.5B	73.40% \pm 4.23	70.67% \pm 4.05	72.48% \pm 4.16	71.46% \pm 4.12	70.20% \pm 4.24	70.77% \pm 4.27
Qwen 3B	73.17% \pm 3.83	69.04% \pm 3.95	72.75% \pm 3.81	72.87% \pm 3.98	68.48% \pm 3.89	72.95% \pm 3.87
Qwen 7B	74.22% \pm 3.52	69.55% \pm 3.78	72.96% \pm 3.69	73.94% \pm 3.69	69.22% \pm 4.08	72.63% \pm 3.72
Qwen 14B	74.86% \pm 3.27	69.10% \pm 3.68	73.18% \pm 3.38	74.73% \pm 3.37	71.11% \pm 3.62	72.94% \pm 3.48
Qwen 32B	76.50% \pm 3.07	69.62% \pm 3.64	73.22% \pm 3.28	76.26% \pm 2.95	72.94% \pm 3.44	75.47% \pm 3.15
Qwen 72B	79.57% \pm 2.54	69.68% \pm 3.66	74.78% \pm 3.36	76.62% \pm 3.06	71.35% \pm 3.71	76.18% \pm 3.36
Llama 8B	73.27% \pm 3.69	75.51% \pm 2.39	74.03% \pm 3.56	74.51% \pm 3.55	70.98% \pm 4.02	71.60% \pm 4.17
Llama 70B	76.37% \pm 3.22	71.22% \pm 3.52	77.52% \pm 2.58	75.51% \pm 3.05	72.90% \pm 3.51	76.19% \pm 3.28
DeepSeekV3	75.76% \pm 3.54	70.13% \pm 3.62	73.24% \pm 3.45	78.82% \pm 2.52	73.35% \pm 3.62	75.97% \pm 3.22
GPT-4o Mini	76.20% \pm 3.44	68.34% \pm 4.09	73.39% \pm 3.71	76.63% \pm 3.48	70.62% \pm 3.26	76.11% \pm 3.36
GPT-4o	76.07% \pm 3.70	68.22% \pm 4.21	72.60% \pm 3.84	76.87% \pm 3.42	67.41% \pm 4.05	71.38% \pm 3.50

Table 18: Accuracy of proxy Kernel SHAP explanations on high school computer science of MMLU datasets: each value shows how well Kernel SHAP explanations generated by the model on the **left** serve as surrogates for predicting the behavior of the model on the **top**.

	Qwen 0.5B	Qwen 1.5B	Qwen 3B	Qwen 7B	Qwen 14B	Qwen 32B
Qwen 0.5B	78.94% ± 3.20	62.47% ± 5.17	61.97% ± 4.79	60.71% ± 5.16	57.75% ± 5.15	59.20% ± 5.11
Qwen 1.5B	61.14% ± 5.59	75.69% ± 3.63	67.03% ± 4.79	69.18% ± 4.81	66.45% ± 4.79	64.11% ± 5.07
Qwen 3B	61.63% ± 5.22	66.26% ± 4.49	72.73% ± 3.81	70.34% ± 4.33	69.87% ± 4.28	70.31% ± 4.45
Qwen 7B	59.00% ± 5.40	64.09% ± 4.69	66.83% ± 4.46	73.20% ± 3.74	70.19% ± 4.11	71.18% ± 3.85
Qwen 14B	59.04% ± 5.47	64.16% ± 4.84	69.60% ± 4.20	73.69% ± 3.97	74.34% ± 4.09	75.84% ± 3.90
Qwen 32B	52.86% ± 3.93	57.94% ± 3.56	59.09% ± 3.25	61.35% ± 3.16	62.02% ± 3.14	62.40% ± 3.19
Qwen 72B	58.06% ± 5.49	62.79% ± 5.17	67.77% ± 4.36	72.77% ± 3.81	71.57% ± 4.26	75.13% ± 3.71
Llama 8B	58.28% ± 5.67	61.59% ± 5.23	65.50% ± 4.66	69.26% ± 4.88	67.55% ± 4.79	66.63% ± 4.97
Llama 70B	59.01% ± 5.86	63.51% ± 5.09	66.50% ± 4.82	72.90% ± 4.03	70.47% ± 4.80	74.90% ± 3.85
DeepSeekV3	57.81% ± 5.77	63.22% ± 5.06	65.30% ± 4.63	71.31% ± 4.37	70.73% ± 4.64	72.04% ± 4.52
GPT-4o Mini	61.37% ± 5.48	64.37% ± 5.01	65.37% ± 4.69	69.66% ± 4.45	69.46% ± 4.59	71.12% ± 4.35
GPT-4o	57.59% ± 5.84	59.38% ± 5.61	62.93% ± 5.11	66.82% ± 4.81	66.55% ± 5.28	69.07% ± 4.86

	Qwen 72B	Llama 8B	Llama 70B	DeepSeekV3	GPT-4o Mini	GPT-4o
Qwen 0.5B	58.02% ± 5.28	61.61% ± 4.81	59.14% ± 5.15	59.99% ± 5.43	58.67% ± 5.54	56.69% ± 5.79
Qwen 1.5B	64.27% ± 5.10	65.30% ± 4.85	66.07% ± 5.04	64.62% ± 5.30	63.27% ± 5.14	62.28% ± 5.79
Qwen 3B	69.72% ± 4.47	66.63% ± 4.25	70.84% ± 4.17	68.22% ± 4.68	68.25% ± 4.33	66.74% ± 4.94
Qwen 7B	70.50% ± 4.10	66.03% ± 4.51	70.67% ± 3.91	69.92% ± 4.22	67.35% ± 4.24	67.61% ± 4.51
Qwen 14B	74.06% ± 4.09	68.61% ± 4.54	73.41% ± 4.03	72.76% ± 4.58	70.20% ± 4.68	70.67% ± 5.02
Qwen 32B	61.44% ± 3.21	59.41% ± 3.39	59.63% ± 3.34	60.41% ± 3.30	58.72% ± 3.43	59.49% ± 3.61
Qwen 72B	75.60% ± 3.57	66.92% ± 4.47	74.79% ± 3.85	72.75% ± 4.19	67.75% ± 4.81	71.22% ± 4.47
Llama 8B	67.39% ± 4.82	70.03% ± 4.27	68.70% ± 4.71	66.92% ± 5.15	65.75% ± 5.04	65.16% ± 5.42
Llama 70B	72.76% ± 4.30	67.10% ± 4.77	76.91% ± 3.65	71.63% ± 4.53	66.94% ± 4.91	67.30% ± 5.31
DeepSeekV3	70.78% ± 4.60	66.43% ± 4.68	72.68% ± 4.19	75.02% ± 4.14	67.05% ± 5.06	68.70% ± 4.94
GPT-4o Mini	70.65% ± 4.48	63.73% ± 4.97	70.58% ± 4.52	71.24% ± 4.72	70.29% ± 4.94	73.27% ± 4.72
GPT-4o	68.38% ± 4.88	62.70% ± 5.13	68.84% ± 4.76	69.57% ± 4.81	67.85% ± 5.19	68.19% ± 5.62

Table 19: Accuracy of **filtered** proxy Kernel SHAP explanations on high school computer science of MMLU datasets: each value shows how well Kernel SHAP explanations generated by the model on the **left** serve as surrogates for predicting the behavior of the model on the **top**.

	Qwen 0.5B	Qwen 1.5B	Qwen 3B	Qwen 7B	Qwen 14B	Qwen 32B
Qwen 0.5B	78.94% \pm 3.20	73.30% \pm 5.79	71.40% \pm 5.84	69.41% \pm 7.09	68.97% \pm 7.31	55.29% \pm 7.38
Qwen 1.5B	71.83% \pm 6.37	75.69% \pm 3.63	72.60% \pm 5.37	75.67% \pm 5.13	73.31% \pm 5.45	64.04% \pm 8.61
Qwen 3B	71.80% \pm 5.76	69.96% \pm 4.74	72.73% \pm 3.81	71.95% \pm 5.08	73.40% \pm 5.04	64.50% \pm 7.61
Qwen 7B	69.11% \pm 6.31	70.92% \pm 5.00	70.42% \pm 5.09	73.20% \pm 3.74	71.46% \pm 4.58	69.11% \pm 6.32
Qwen 14B	72.27% \pm 6.55	72.50% \pm 4.98	74.73% \pm 4.58	75.39% \pm 4.35	74.34% \pm 4.09	70.47% \pm 7.47
Qwen 32B	51.87% \pm 5.21	56.86% \pm 5.96	55.80% \pm 5.37	62.33% \pm 5.40	62.89% \pm 5.26	62.40% \pm 3.19
Qwen 72B	69.31% \pm 6.79	71.64% \pm 4.91	73.27% \pm 4.65	73.26% \pm 4.22	72.96% \pm 4.36	70.74% \pm 7.97
Llama 8B	70.88% \pm 7.60	68.47% \pm 5.71	69.63% \pm 5.30	71.86% \pm 5.62	71.08% \pm 5.52	70.90% \pm 9.64
Llama 70B	72.58% \pm 7.02	72.12% \pm 5.19	71.33% \pm 5.39	73.48% \pm 4.43	71.71% \pm 5.06	70.92% \pm 7.83
DeepSeekV3	70.49% \pm 6.87	70.88% \pm 5.81	71.81% \pm 5.28	72.24% \pm 4.78	72.83% \pm 4.88	64.75% \pm 10.47
GPT-4o Mini	72.76% \pm 6.06	70.58% \pm 5.45	67.45% \pm 5.54	68.70% \pm 4.94	70.37% \pm 5.31	65.80% \pm 8.57
GPT-4o	66.78% \pm 7.81	67.19% \pm 6.41	67.48% \pm 5.96	66.75% \pm 5.38	68.45% \pm 5.80	63.02% \pm 10.25

	Qwen 72B	Llama 8B	Llama 70B	DeepSeekV3	GPT-4o Mini	GPT-4o
Qwen 0.5B	71.58% \pm 7.33	74.66% \pm 5.72	73.57% \pm 6.62	72.41% \pm 6.97	70.12% \pm 7.96	69.07% \pm 8.17
Qwen 1.5B	74.25% \pm 5.43	70.00% \pm 5.28	76.48% \pm 4.87	74.20% \pm 5.79	70.73% \pm 5.87	71.90% \pm 5.99
Qwen 3B	75.19% \pm 4.98	68.55% \pm 4.55	75.98% \pm 4.51	72.74% \pm 5.35	70.15% \pm 5.05	70.90% \pm 5.56
Qwen 7B	72.87% \pm 4.21	68.78% \pm 4.96	73.73% \pm 3.91	70.59% \pm 4.58	69.56% \pm 4.42	69.18% \pm 4.71
Qwen 14B	76.00% \pm 4.26	72.38% \pm 4.76	75.07% \pm 4.29	74.14% \pm 4.85	72.73% \pm 5.03	72.81% \pm 5.28
Qwen 32B	57.79% \pm 5.32	58.29% \pm 6.01	56.93% \pm 5.67	56.43% \pm 5.26	54.72% \pm 5.83	51.39% \pm 6.52
Qwen 72B	75.60% \pm 3.57	70.47% \pm 4.84	76.41% \pm 3.73	72.85% \pm 4.30	70.26% \pm 5.10	73.12% \pm 4.38
Llama 8B	73.38% \pm 5.18	70.03% \pm 4.27	74.60% \pm 4.82	73.29% \pm 5.45	71.20% \pm 5.49	72.36% \pm 5.78
Llama 70B	74.03% \pm 4.32	70.60% \pm 5.08	76.91% \pm 3.65	72.43% \pm 4.70	69.47% \pm 5.37	69.39% \pm 5.41
DeepSeekV3	73.10% \pm 4.47	70.67% \pm 4.93	74.34% \pm 4.31	75.02% \pm 4.14	69.91% \pm 5.42	70.21% \pm 5.05
GPT-4o Mini	72.01% \pm 4.89	66.35% \pm 5.47	72.84% \pm 4.79	72.13% \pm 5.04	70.29% \pm 4.94	73.04% \pm 5.12
GPT-4o	70.42% \pm 5.11	64.97% \pm 6.24	71.37% \pm 4.94	69.83% \pm 5.19	69.41% \pm 5.72	68.19% \pm 5.62

Table 20: Accuracy of proxy Kernel SHAP explanations on high school microeconomics of MMLU datasets: each value shows how well Kernel SHAP explanations generated by the model on the **left** serve as surrogates for predicting the behavior of the model on the **top**.

	Qwen 0.5B	Qwen 1.5B	Qwen 3B	Qwen 7B	Qwen 14B	Qwen 32B
Qwen 0.5B	80.88% ± 1.98	61.67% ± 3.43	57.45% ± 3.41	56.32% ± 3.82	55.58% ± 3.69	53.73% ± 3.81
Qwen 1.5B	59.47% ± 3.52	78.61% ± 2.28	67.09% ± 3.10	67.26% ± 3.49	66.60% ± 3.40	65.98% ± 3.54
Qwen 3B	55.26% ± 3.61	66.02% ± 3.26	78.10% ± 2.23	71.28% ± 3.05	70.98% ± 2.92	69.09% ± 3.14
Qwen 7B	55.17% ± 3.72	64.23% ± 3.41	68.50% ± 3.05	81.79% ± 2.08	73.68% ± 2.80	76.07% ± 2.62
Qwen 14B	54.66% ± 3.65	62.56% ± 3.40	67.67% ± 3.11	74.66% ± 2.69	78.87% ± 2.32	76.76% ± 2.54
Qwen 32B	54.25% ± 3.72	62.40% ± 3.54	67.24% ± 3.11	74.79% ± 2.79	75.49% ± 2.60	81.67% ± 2.20
Qwen 72B	53.16% ± 3.66	62.17% ± 3.39	66.47% ± 3.11	74.49% ± 2.73	75.05% ± 2.64	78.53% ± 2.39
Llama 8B	57.76% ± 3.53	65.09% ± 3.13	67.47% ± 3.08	70.17% ± 3.25	70.40% ± 3.11	69.81% ± 3.24
Llama 70B	54.42% ± 3.74	63.87% ± 3.35	67.13% ± 3.13	74.33% ± 2.80	74.19% ± 2.84	75.99% ± 2.65
DeepSeekV3	52.79% ± 3.83	60.88% ± 3.69	65.88% ± 3.38	73.14% ± 3.13	75.08% ± 2.89	77.05% ± 2.60
GPT-4o Mini	53.87% ± 3.73	63.73% ± 3.39	66.83% ± 3.12	73.03% ± 2.92	74.01% ± 2.84	76.38% ± 2.66
GPT-4o	54.03% ± 3.75	61.93% ± 3.45	65.49% ± 3.25	74.17% ± 2.77	74.12% ± 2.84	76.34% ± 2.73

	Qwen 72B	Llama 8B	Llama 70B	DeepSeekV3	GPT-4o Mini	GPT-4o
Qwen 0.5B	53.40% ± 4.00	58.72% ± 3.55	55.39% ± 3.84	53.12% ± 4.06	55.12% ± 3.69	52.46% ± 4.02
Qwen 1.5B	66.36% ± 3.71	68.09% ± 3.14	68.17% ± 3.39	66.08% ± 3.75	66.93% ± 3.39	65.83% ± 3.65
Qwen 3B	68.05% ± 3.31	67.25% ± 3.17	69.07% ± 3.11	67.31% ± 3.44	68.98% ± 3.05	66.96% ± 3.34
Qwen 7B	74.55% ± 2.79	68.18% ± 3.26	73.19% ± 2.83	75.48% ± 2.80	72.01% ± 2.88	74.11% ± 2.79
Qwen 14B	75.63% ± 2.75	66.99% ± 3.29	74.03% ± 2.78	76.79% ± 2.74	74.61% ± 2.74	75.21% ± 2.78
Qwen 32B	77.35% ± 2.73	67.79% ± 3.21	75.45% ± 2.78	79.40% ± 2.52	74.20% ± 2.80	76.72% ± 2.74
Qwen 72B	83.40% ± 2.03	66.96% ± 3.16	76.92% ± 2.69	80.37% ± 2.41	74.94% ± 2.78	79.23% ± 2.60
Llama 8B	69.87% ± 3.30	79.76% ± 2.22	71.90% ± 3.08	70.37% ± 3.42	69.59% ± 3.23	70.53% ± 3.33
Llama 70B	78.62% ± 2.61	69.43% ± 3.08	82.66% ± 2.07	79.18% ± 2.59	75.73% ± 2.73	79.34% ± 2.41
DeepSeekV3	79.11% ± 2.66	66.97% ± 3.38	75.74% ± 2.83	83.59% ± 2.14	73.88% ± 3.01	77.08% ± 2.83
GPT-4o Mini	77.49% ± 2.75	67.53% ± 3.24	76.78% ± 2.75	77.97% ± 2.73	79.43% ± 2.52	79.36% ± 2.53
GPT-4o	78.36% ± 2.74	67.54% ± 3.14	76.75% ± 2.66	78.82% ± 2.70	75.37% ± 2.78	82.00% ± 2.28

Table 21: Accuracy of **filtered** proxy Kernel SHAP explanations on high school microeconomics of MMLU datasets: each value shows how well Kernel SHAP explanations generated by the model on the **left** serve as surrogates for predicting the behavior of the model on the **top**.

	Qwen 0.5B	Qwen 1.5B	Qwen 3B	Qwen 7B	Qwen 14B	Qwen 32B
Qwen 0.5B	80.88% ± 1.98	71.51% ± 3.83	70.03% ± 3.99	76.19% ± 3.64	72.03% ± 4.20	73.52% ± 3.93
Qwen 1.5B	74.25% ± 3.36	78.61% ± 2.28	73.88% ± 3.15	77.99% ± 2.82	76.05% ± 2.98	76.95% ± 2.92
Qwen 3B	71.52% ± 3.73	73.73% ± 2.98	78.10% ± 2.23	76.84% ± 2.73	76.58% ± 2.71	76.12% ± 2.89
Qwen 7B	73.92% ± 3.80	74.14% ± 2.88	73.50% ± 3.05	81.79% ± 2.08	75.55% ± 2.89	78.63% ± 2.53
Qwen 14B	71.25% ± 4.05	71.35% ± 3.12	73.77% ± 3.05	77.18% ± 2.59	78.87% ± 2.32	78.78% ± 2.49
Qwen 32B	72.83% ± 3.91	71.94% ± 3.23	73.06% ± 3.15	77.82% ± 2.60	76.94% ± 2.69	81.67% ± 2.20
Qwen 72B	69.76% ± 4.10	71.24% ± 3.30	71.84% ± 3.19	76.97% ± 2.63	76.58% ± 2.63	79.73% ± 2.36
Llama 8B	73.29% ± 3.71	70.83% ± 3.17	73.58% ± 3.25	77.27% ± 2.80	76.30% ± 2.86	77.08% ± 2.83
Llama 70B	72.80% ± 4.00	72.09% ± 3.18	72.05% ± 3.20	77.04% ± 2.60	76.71% ± 2.69	77.80% ± 2.54
DeepSeekV3	72.04% ± 4.14	71.02% ± 3.52	72.49% ± 3.37	76.66% ± 2.95	77.72% ± 2.72	78.28% ± 2.62
GPT-4o Mini	71.23% ± 4.08	72.52% ± 3.26	71.57% ± 3.24	76.25% ± 2.72	76.56% ± 2.78	78.77% ± 2.53
GPT-4o	71.55% ± 4.17	70.04% ± 3.38	70.92% ± 3.39	76.52% ± 2.80	76.10% ± 2.79	78.07% ± 2.61

	Qwen 72B	Llama 8B	Llama 70B	DeepSeekV3	GPT-4o Mini	GPT-4o
Qwen 0.5B	74.58% ± 3.94	71.47% ± 3.96	74.22% ± 3.98	75.53% ± 4.09	70.43% ± 4.34	74.36% ± 4.17
Qwen 1.5B	78.92% ± 2.95	74.80% ± 2.91	78.25% ± 2.90	79.15% ± 2.79	76.23% ± 3.13	77.51% ± 2.93
Qwen 3B	76.03% ± 2.77	75.34% ± 2.82	75.43% ± 2.83	76.00% ± 2.93	73.94% ± 2.94	74.93% ± 2.87
Qwen 7B	77.57% ± 2.55	74.54% ± 3.00	76.10% ± 2.73	78.93% ± 2.54	74.64% ± 2.76	77.81% ± 2.50
Qwen 14B	78.32% ± 2.48	73.55% ± 3.06	76.81% ± 2.64	79.37% ± 2.53	76.87% ± 2.63	78.06% ± 2.50
Qwen 32B	79.46% ± 2.52	73.53% ± 3.12	77.78% ± 2.62	80.74% ± 2.46	76.27% ± 2.80	78.95% ± 2.50
Qwen 72B	83.40% ± 2.03	72.58% ± 3.05	79.72% ± 2.43	81.16% ± 2.36	77.04% ± 2.60	81.20% ± 2.28
Llama 8B	78.18% ± 2.73	79.76% ± 2.22	79.26% ± 2.65	79.66% ± 2.78	76.04% ± 3.07	78.93% ± 2.73
Llama 70B	81.90% ± 2.15	75.09% ± 2.88	82.66% ± 2.07	81.63% ± 2.29	77.56% ± 2.67	81.42% ± 2.17
DeepSeekV3	80.79% ± 2.46	73.96% ± 3.22	78.81% ± 2.57	83.59% ± 2.14	76.16% ± 2.89	78.81% ± 2.57
GPT-4o Mini	80.57% ± 2.39	74.43% ± 3.02	79.33% ± 2.52	80.78% ± 2.41	79.43% ± 2.52	81.61% ± 2.29
GPT-4o	80.38% ± 2.54	73.15% ± 3.07	78.49% ± 2.60	79.92% ± 2.59	76.48% ± 2.83	82.00% ± 2.28

Table 22: Accuracy of proxy Kernel SHAP explanations on high school psychology of MMLU datasets: each value shows how well Kernel SHAP explanations generated by the model on the **left** serve as surrogates for predicting the behavior of the model on the **top**.

	Qwen 0.5B	Qwen 1.5B	Qwen 3B	Qwen 7B	Qwen 14B	Qwen 32B
Qwen 0.5B	79.08% \pm 1.31	65.63% \pm 2.05	63.79% \pm 1.97	63.02% \pm 2.13	62.30% \pm 2.21	61.41% \pm 2.22
Qwen 1.5B	63.83% \pm 2.05	79.61% \pm 1.33	72.62% \pm 1.61	74.60% \pm 1.57	73.54% \pm 1.69	73.37% \pm 1.72
Qwen 3B	59.66% \pm 2.05	69.23% \pm 1.78	75.48% \pm 1.39	71.30% \pm 1.65	71.97% \pm 1.67	71.63% \pm 1.67
Qwen 7B	60.72% \pm 2.05	69.35% \pm 1.68	69.59% \pm 1.62	77.64% \pm 1.38	74.26% \pm 1.56	74.20% \pm 1.57
Qwen 14B	60.05% \pm 2.02	67.38% \pm 1.77	69.23% \pm 1.61	71.54% \pm 1.63	76.59% \pm 1.47	74.28% \pm 1.56
Qwen 32B	60.12% \pm 2.11	68.44% \pm 1.87	70.53% \pm 1.68	74.64% \pm 1.63	77.50% \pm 1.52	80.23% \pm 1.32
Qwen 72B	59.83% \pm 2.10	68.97% \pm 1.82	70.05% \pm 1.65	74.23% \pm 1.55	76.04% \pm 1.51	76.85% \pm 1.44
Llama 8B	60.67% \pm 2.12	70.39% \pm 1.84	71.71% \pm 1.66	74.68% \pm 1.68	75.20% \pm 1.66	76.18% \pm 1.54
Llama 70B	59.80% \pm 2.24	68.78% \pm 1.98	70.36% \pm 1.77	74.87% \pm 1.68	77.40% \pm 1.59	78.88% \pm 1.45
DeepSeekV3	58.41% \pm 2.18	68.47% \pm 1.86	69.13% \pm 1.71	73.91% \pm 1.67	75.53% \pm 1.58	76.85% \pm 1.55
GPT-4o Mini	58.81% \pm 2.25	68.85% \pm 2.07	71.60% \pm 1.84	74.71% \pm 1.83	77.66% \pm 1.70	79.52% \pm 1.53
GPT-4o	58.61% \pm 2.30	67.57% \pm 2.18	71.37% \pm 1.85	75.03% \pm 1.83	77.62% \pm 1.70	79.46% \pm 1.60

	Qwen 72B	Llama 8B	Llama 70B	DeepSeekV3	GPT-4o Mini	GPT-4o
Qwen 0.5B	60.79% \pm 2.38	62.77% \pm 2.13	60.61% \pm 2.37	59.51% \pm 2.44	60.85% \pm 2.32	58.50% \pm 2.48
Qwen 1.5B	74.23% \pm 1.81	72.89% \pm 1.69	73.18% \pm 1.85	73.22% \pm 1.94	71.95% \pm 1.89	71.72% \pm 2.04
Qwen 3B	71.15% \pm 1.77	71.08% \pm 1.69	70.79% \pm 1.79	70.66% \pm 1.83	71.15% \pm 1.70	70.03% \pm 1.82
Qwen 7B	73.62% \pm 1.66	71.53% \pm 1.69	73.36% \pm 1.67	73.32% \pm 1.75	71.54% \pm 1.75	72.46% \pm 1.80
Qwen 14B	73.32% \pm 1.64	70.07% \pm 1.71	72.94% \pm 1.69	72.48% \pm 1.75	72.09% \pm 1.73	72.53% \pm 1.78
Qwen 32B	78.74% \pm 1.46	72.96% \pm 1.69	78.28% \pm 1.50	77.95% \pm 1.59	75.94% \pm 1.65	77.78% \pm 1.64
Qwen 72B	80.22% \pm 1.36	72.10% \pm 1.71	77.50% \pm 1.53	78.20% \pm 1.51	74.52% \pm 1.73	76.43% \pm 1.65
Llama 8B	75.64% \pm 1.71	80.42% \pm 1.30	76.43% \pm 1.65	75.65% \pm 1.74	74.70% \pm 1.75	74.73% \pm 1.85
Llama 70B	79.82% \pm 1.49	74.16% \pm 1.70	83.22% \pm 1.29	79.27% \pm 1.60	78.07% \pm 1.62	79.35% \pm 1.61
DeepSeekV3	78.67% \pm 1.49	72.02% \pm 1.70	77.18% \pm 1.63	81.20% \pm 1.44	74.70% \pm 1.76	77.06% \pm 1.71
GPT-4o Mini	80.95% \pm 1.59	74.53% \pm 1.84	80.55% \pm 1.64	81.44% \pm 1.63	82.88% \pm 1.50	81.75% \pm 1.56
GPT-4o	81.79% \pm 1.54	73.65% \pm 1.92	80.76% \pm 1.69	82.81% \pm 1.51	79.56% \pm 1.67	84.90% \pm 1.39

Table 23: Accuracy of **filtered** proxy Kernel SHAP explanations on high school psychology of MMLU datasets: each value shows how well Kernel SHAP explanations generated by the model on the **left** serve as surrogates for predicting the behavior of the model on the **top**.

	Qwen 0.5B	Qwen 1.5B	Qwen 3B	Qwen 7B	Qwen 14B	Qwen 32B
Qwen 0.5B	79.08% ± 1.31	74.22% ± 1.95	72.93% ± 1.87	74.33% ± 1.83	74.51% ± 1.99	74.74% ± 1.92
Qwen 1.5B	71.53% ± 2.08	79.61% ± 1.33	75.67% ± 1.54	77.69% ± 1.46	77.34% ± 1.58	77.96% ± 1.53
Qwen 3B	67.79% ± 2.10	72.71% ± 1.68	75.48% ± 1.39	73.61% ± 1.56	74.67% ± 1.54	74.65% ± 1.56
Qwen 7B	68.82% ± 2.03	72.49% ± 1.63	71.43% ± 1.60	77.64% ± 1.38	75.88% ± 1.46	76.06% ± 1.47
Qwen 14B	68.01% ± 2.08	71.32% ± 1.68	71.58% ± 1.61	73.57% ± 1.55	76.59% ± 1.47	75.41% ± 1.56
Qwen 32B	68.95% ± 2.20	72.59% ± 1.82	73.47% ± 1.66	76.69% ± 1.58	78.71% ± 1.49	80.23% ± 1.32
Qwen 72B	67.71% ± 2.22	72.93% ± 1.74	73.09% ± 1.60	76.02% ± 1.47	77.49% ± 1.48	77.89% ± 1.38
Llama 8B	68.90% ± 2.22	74.14% ± 1.80	74.68% ± 1.63	77.49% ± 1.56	78.30% ± 1.53	79.23% ± 1.39
Llama 70B	69.71% ± 2.34	73.84% ± 1.85	73.70% ± 1.73	77.59% ± 1.55	79.26% ± 1.50	79.94% ± 1.40
DeepSeekV3	66.84% ± 2.25	72.66% ± 1.82	72.10% ± 1.72	75.88% ± 1.60	77.05% ± 1.53	78.14% ± 1.47
GPT-4o Mini	68.49% ± 2.40	74.08% ± 1.93	74.62% ± 1.81	77.38% ± 1.70	79.86% ± 1.59	81.34% ± 1.41
GPT-4o	67.44% ± 2.51	73.06% ± 2.08	74.54% ± 1.85	77.72% ± 1.72	79.61% ± 1.65	81.15% ± 1.47

	Qwen 72B	Llama 8B	Llama 70B	DeepSeekV3	GPT-4o Mini	GPT-4o
Qwen 0.5B	75.51% ± 1.92	73.90% ± 1.98	75.32% ± 1.96	74.36% ± 2.01	74.99% ± 1.93	74.59% ± 2.06
Qwen 1.5B	79.37% ± 1.53	76.60% ± 1.60	78.11% ± 1.60	79.03% ± 1.62	77.55% ± 1.63	78.58% ± 1.61
Qwen 3B	74.62% ± 1.61	74.37% ± 1.60	74.32% ± 1.62	74.70% ± 1.67	74.17% ± 1.57	74.33% ± 1.64
Qwen 7B	75.52% ± 1.54	74.00% ± 1.63	75.52% ± 1.57	75.61% ± 1.61	74.25% ± 1.56	75.82% ± 1.59
Qwen 14B	74.74% ± 1.64	72.66% ± 1.69	74.33% ± 1.67	74.16% ± 1.68	74.20% ± 1.60	75.02% ± 1.65
Qwen 32B	79.76% ± 1.41	75.96% ± 1.63	79.07% ± 1.51	79.39% ± 1.48	77.99% ± 1.49	79.70% ± 1.47
Qwen 72B	80.22% ± 1.36	74.88% ± 1.68	78.28% ± 1.51	78.84% ± 1.49	76.69% ± 1.52	77.78% ± 1.53
Llama 8B	79.35% ± 1.49	80.42% ± 1.30	79.59% ± 1.49	79.22% ± 1.49	78.34% ± 1.49	79.08% ± 1.55
Llama 70B	81.02% ± 1.40	77.30% ± 1.64	83.22% ± 1.29	80.92% ± 1.48	80.10% ± 1.41	81.31% ± 1.41
DeepSeekV3	79.29% ± 1.49	74.58% ± 1.67	78.34% ± 1.58	81.20% ± 1.44	76.84% ± 1.57	78.42% ± 1.58
GPT-4o Mini	82.86% ± 1.43	77.76% ± 1.77	82.32% ± 1.49	83.53% ± 1.43	82.88% ± 1.50	83.21% ± 1.43
GPT-4o	83.03% ± 1.42	77.11% ± 1.84	82.22% ± 1.56	83.76% ± 1.45	81.02% ± 1.57	84.90% ± 1.39

Table 24: Accuracy of proxy Kernel SHAP explanations on high school world history of MMLU datasets: each value shows how well Kernel SHAP explanations generated by the model on the **left** serve as surrogates for predicting the behavior of the model on the **top**.

	Qwen 0.5B	Qwen 1.5B	Qwen 3B	Qwen 7B	Qwen 14B	Qwen 32B
Qwen 0.5B	72.40% \pm 2.05	62.35% \pm 2.94	59.56% \pm 3.24	60.02% \pm 3.37	59.10% \pm 3.42	57.78% \pm 3.57
Qwen 1.5B	60.54% \pm 2.90	71.46% \pm 2.21	66.05% \pm 2.75	64.90% \pm 2.85	65.14% \pm 2.98	64.04% \pm 3.11
Qwen 3B	57.08% \pm 3.00	63.65% \pm 2.78	69.47% \pm 2.53	66.65% \pm 2.70	67.13% \pm 2.85	65.96% \pm 3.00
Qwen 7B	57.38% \pm 3.22	63.31% \pm 2.95	65.71% \pm 2.78	69.57% \pm 2.58	68.18% \pm 2.77	67.32% \pm 2.88
Qwen 14B	57.35% \pm 3.19	61.86% \pm 3.11	65.27% \pm 2.96	67.56% \pm 2.87	70.78% \pm 2.75	69.59% \pm 2.89
Qwen 32B	59.10% \pm 3.23	63.17% \pm 3.17	66.26% \pm 3.02	70.14% \pm 2.82	73.02% \pm 2.72	73.87% \pm 2.68
Qwen 72B	59.32% \pm 3.36	63.77% \pm 3.26	68.47% \pm 3.07	70.72% \pm 2.87	73.89% \pm 2.72	74.45% \pm 2.81
Llama 8B	59.53% \pm 3.05	64.20% \pm 2.79	68.15% \pm 2.66	69.40% \pm 2.56	71.08% \pm 2.51	71.23% \pm 2.54
Llama 70B	60.00% \pm 3.40	63.85% \pm 3.35	68.61% \pm 3.08	71.83% \pm 2.83	75.21% \pm 2.66	75.08% \pm 2.75
DeepSeekV3	59.74% \pm 3.57	65.58% \pm 3.40	68.28% \pm 3.28	71.61% \pm 2.97	74.67% \pm 2.88	74.50% \pm 2.94
GPT-4o Mini	59.78% \pm 3.31	64.68% \pm 3.17	67.96% \pm 2.93	71.22% \pm 2.80	73.81% \pm 2.66	73.81% \pm 2.78
GPT-4o	59.88% \pm 3.45	64.76% \pm 3.37	68.83% \pm 3.18	73.11% \pm 2.86	76.28% \pm 2.67	76.22% \pm 2.76

	Qwen 72B	Llama 8B	Llama 70B	DeepSeekV3	GPT-4o Mini	GPT-4o
Qwen 0.5B	57.37% \pm 3.66	57.92% \pm 3.39	56.94% \pm 3.60	57.64% \pm 3.71	58.07% \pm 3.58	56.82% \pm 3.78
Qwen 1.5B	63.60% \pm 3.31	63.93% \pm 3.00	62.70% \pm 3.19	64.44% \pm 3.31	63.97% \pm 3.20	62.38% \pm 3.43
Qwen 3B	65.84% \pm 3.11	65.85% \pm 2.83	64.87% \pm 3.09	65.27% \pm 3.18	65.55% \pm 2.95	65.44% \pm 3.20
Qwen 7B	67.86% \pm 2.96	66.24% \pm 2.85	66.17% \pm 2.97	67.30% \pm 3.02	66.50% \pm 3.01	67.81% \pm 2.96
Qwen 14B	69.76% \pm 3.00	65.89% \pm 2.95	68.90% \pm 2.97	69.73% \pm 2.99	68.22% \pm 2.96	70.00% \pm 3.04
Qwen 32B	72.97% \pm 2.87	68.77% \pm 2.94	71.51% \pm 2.92	72.60% \pm 2.90	71.18% \pm 2.87	72.93% \pm 2.94
Qwen 72B	76.75% \pm 2.69	69.72% \pm 3.06	74.91% \pm 2.80	74.89% \pm 2.87	73.34% \pm 2.86	75.99% \pm 2.85
Llama 8B	71.62% \pm 2.74	72.90% \pm 2.34	70.23% \pm 2.76	70.89% \pm 2.81	69.83% \pm 2.76	70.73% \pm 2.87
Llama 70B	76.64% \pm 2.69	71.32% \pm 2.98	78.17% \pm 2.49	77.25% \pm 2.66	74.90% \pm 2.78	78.10% \pm 2.60
DeepSeekV3	76.17% \pm 2.91	70.64% \pm 3.15	75.11% \pm 2.91	78.56% \pm 2.75	74.02% \pm 2.95	77.89% \pm 2.82
GPT-4o Mini	75.06% \pm 2.73	70.99% \pm 2.82	74.50% \pm 2.74	75.02% \pm 2.74	75.64% \pm 2.61	75.44% \pm 2.78
GPT-4o	78.32% \pm 2.70	72.02% \pm 3.01	76.65% \pm 2.78	78.78% \pm 2.66	75.69% \pm 2.80	80.01% \pm 2.60

Table 25: Accuracy of **filtered** proxy Kernel SHAP explanations on high school world history of MMLU datasets: each value shows how well Kernel SHAP explanations generated by the model on the **left** serve as surrogates for predicting the behavior of the model on the **top**.

	Qwen 0.5B	Qwen 1.5B	Qwen 3B	Qwen 7B	Qwen 14B	Qwen 32B
Qwen 0.5B	72.40% ± 2.05	69.14% ± 3.13	67.89% ± 3.27	68.97% ± 3.25	70.98% ± 3.15	71.14% ± 3.17
Qwen 1.5B	66.58% ± 3.17	71.46% ± 2.21	68.56% ± 2.84	69.61% ± 2.97	70.99% ± 2.91	70.67% ± 2.88
Qwen 3B	63.13% ± 3.33	67.12% ± 2.93	69.47% ± 2.53	67.74% ± 2.89	69.78% ± 2.99	69.41% ± 3.01
Qwen 7B	65.07% ± 3.33	68.07% ± 2.98	66.88% ± 2.91	69.57% ± 2.58	69.82% ± 2.81	69.69% ± 2.87
Qwen 14B	65.76% ± 3.52	67.57% ± 3.23	67.93% ± 3.12	69.01% ± 3.01	70.78% ± 2.75	71.04% ± 2.96
Qwen 32B	67.16% ± 3.43	68.75% ± 3.20	69.01% ± 3.13	71.31% ± 2.97	73.79% ± 2.82	73.87% ± 2.68
Qwen 72B	68.43% ± 3.40	70.73% ± 3.18	71.74% ± 3.07	72.86% ± 2.93	76.04% ± 2.73	76.19% ± 2.85
Llama 8B	67.43% ± 3.08	68.96% ± 2.83	69.79% ± 2.73	71.56% ± 2.66	73.38% ± 2.60	73.31% ± 2.57
Llama 70B	69.79% ± 3.46	71.62% ± 3.15	72.45% ± 3.07	73.81% ± 2.87	77.56% ± 2.65	77.43% ± 2.67
DeepSeekV3	69.40% ± 3.60	73.27% ± 3.20	71.65% ± 3.33	73.29% ± 3.05	76.57% ± 2.92	75.87% ± 2.98
GPT-4o Mini	68.42% ± 3.34	71.10% ± 3.19	70.72% ± 2.99	73.15% ± 2.84	75.70% ± 2.73	75.83% ± 2.79
GPT-4o	70.26% ± 3.42	71.91% ± 3.23	72.42% ± 3.15	74.68% ± 2.93	78.09% ± 2.71	77.61% ± 2.76

	Qwen 72B	Llama 8B	Llama 70B	DeepSeekV3	GPT-4o Mini	GPT-4o
Qwen 0.5B	70.14% ± 3.28	68.51% ± 3.28	70.02% ± 3.38	71.42% ± 3.29	69.45% ± 3.32	71.82% ± 3.36
Qwen 1.5B	71.28% ± 2.97	69.62% ± 2.99	70.66% ± 2.98	72.63% ± 2.97	70.39% ± 3.11	71.47% ± 3.02
Qwen 3B	69.69% ± 3.05	67.93% ± 2.90	68.83% ± 3.07	69.01% ± 3.11	68.67% ± 2.98	69.69% ± 3.10
Qwen 7B	70.35% ± 2.95	68.64% ± 2.94	68.63% ± 2.96	69.16% ± 3.01	68.93% ± 3.02	70.27% ± 2.92
Qwen 14B	71.77% ± 3.03	68.51% ± 3.06	71.09% ± 3.05	71.56% ± 3.02	70.13% ± 3.06	72.33% ± 3.03
Qwen 32B	74.40% ± 2.93	70.83% ± 3.00	73.21% ± 2.98	73.51% ± 2.97	72.84% ± 2.95	74.54% ± 2.89
Qwen 72B	76.75% ± 2.69	72.92% ± 3.05	75.98% ± 2.85	76.64% ± 2.84	74.83% ± 2.86	77.75% ± 2.81
Llama 8B	74.93% ± 2.61	72.90% ± 2.34	74.10% ± 2.69	74.53% ± 2.71	73.25% ± 2.72	74.71% ± 2.64
Llama 70B	77.93% ± 2.69	75.18% ± 2.89	78.17% ± 2.49	78.06% ± 2.63	76.92% ± 2.70	79.13% ± 2.56
DeepSeekV3	77.54% ± 2.96	74.17% ± 3.14	75.72% ± 2.97	78.56% ± 2.75	75.43% ± 2.95	78.69% ± 2.85
GPT-4o Mini	76.36% ± 2.73	73.80% ± 2.85	75.96% ± 2.80	76.53% ± 2.69	75.64% ± 2.61	77.85% ± 2.73
GPT-4o	79.76% ± 2.66	75.24% ± 2.92	77.41% ± 2.81	79.46% ± 2.69	77.55% ± 2.82	80.01% ± 2.60